AD_____

Award Number: DAMD17-96-1-6280

TITLE: 2-D and 3-D Digital Analysis of Breast Calcifications: A Technique to Improve Mammographic Specificity

PRINCIPAL INVESTIGATOR: Andrew D. Maidment, Ph.D.

CONTRACTING ORGANIZATION: Thomas Jefferson University
Philadelphia, Pennsylvania 19107

REPORT DATE: June 2001

TYPE OF REPORT: Final

PREPARED FOR: U.S. Army Medical Research and Materiel Command
Fort Detrick, Maryland 21702-5012

REPORT DOCUMENTATION PAGE

Form Approved
OMB No. 074-0188

1. AGENCY USE ONLY (Leave blank)	2. REPORT DATE	3. REPORT TYPE AND DATES COVERED
	June 2001	Final (15 Aug 97 - 31 May 01)

4. TITLE AND SUBTITLE
2-D and 3-D Digital Analysis of Breast Calcifications: A Technique to Improve Mammographic Specificity

5. FUNDING NUMBERS
DAMD17-96-1-6280

6. AUTHOR(S):
Andrew D. Maidment, Ph.D.

7. PERFORMING ORGANIZATION NAME(S) AND ADDRESS(ES)
Thomas Jefferson University
Philadelphia, Pennsylvania 19107

E-Mail: Andrew.Maidment@mail.tju.edu

8. PERFORMING ORGANIZATION REPORT NUMBER

9. SPONSORING / MONITORING AGENCY NAME(S) AND ADDRESS(ES)
U.S. Army Medical Research and Materiel Command
Fort Detrick, Maryland 21702-5012

10. SPONSORING / MONITORING AGENCY REPORT NUMBER

11. SUPPLEMENTARY NOTES

12a. DISTRIBUTION / AVAILABILITY STATEMENT
Approved for Public Release; Distribution Unlimited

12b. DISTRIBUTION CODE

13. Abstract ***(Maximum 200 Words)*** *(abstract should contain no proprietary or confidential information)*

A method of imaging breast calcifications in 3D was developed. The method is based upon the principles of limited-view image reconstruction. Each calcification is manually identified in multiple views of the breast, and is then semi-automatically segmented. The identified position in 3D is calculated geometrically. The segmented views of each calcification are used to generate a 3D model of each calcification. The calcifications are rendered with custom viewing software that can render the images stereoscopically. The technique has been shown to be capable of rendering calcifications as small as 100 μm, with an accuracy of approximately 100 μm. A clinical trial was conducted. In instances where calcifications are associated with a mass, we can distinguish preferentially peripherally distributed calcifications from homogeneously distributed calcifications. We have also been able to elucidate the linear distribution of calcifications contained within the ductal system. In an ROC study involving 3 radiologists and 42 cases, we were not able to show a statistically significant difference in Az from viewing calcifications in 3D.

14. SUBJECT TERMS	15. NUMBER OF PAGES
breast cancer, digital mammography, 3-D breast imaging, limited-view image reconstruction, clinical trial	48
	16. PRICE CODE

17. SECURITY CLASSIFICATION OF REPORT	18. SECURITY CLASSIFICATION OF THIS PAGE	19. SECURITY CLASSIFICATION OF ABSTRACT	20. LIMITATION OF ABSTRACT
Unclassified	Unclassified	Unclassified	Unlimited

FOREWORD

Opinions, interpretations, conclusions and recommendations are those of the author and are not necessarily endorsed by the U.S. Army.

N/A Where copyrighted material is quoted, permission has been obtained to use such material.

N/A Where material from documents designated for limited distribution is quoted, permission has been obtained to use the material.

N/A Citations of commercial organizations and trade names in this report do not constitute an official Department of Army endorsement or approval of the products or services of these organizations.

N/A In conducting research using animals, the investigator(s) adhered to the "Guide for the Care and Use of Laboratory Animals," prepared by the Committee on Care and use of Laboratory Animals of the Institute of Laboratory Resources, national Research Council (NIH Publication No. 86-23, Revised 1985).

X For the protection of human subjects, the investigator(s) adhered to policies of applicable Federal Law 45 CFR 46.

N/A In conducting research utilizing recombinant DNA technology, the investigator(s) adhered to current guidelines promulgated by the National Institutes of Health.

N/A In the conduct of research utilizing recombinant DNA, the investigator(s) adhered to the NIH Guidelines for Research Involving Recombinant DNA Molecules.

N/A In the conduct of research involving hazardous organisms, the investigator(s) adhered to the CDC-NIH Guide for Biosafety in Microbiological and Biomedical Laboratories.

9/19/02

PI - Signature Date

Table of Contents

1. Introduction

It has been reported that 29% to 48% of nonpalpable carcinomas are visible on the basis of calcifications alone. Calcifications are especially important as a sign of early breast cancer. Although certain calcifications are pathognomonic of malignant or benign lesions, so that biopsy is definitely indicated or contraindicated, in other instances the appearance is indeterminate, suggesting the possibility of carcinoma to varying degrees. A review of the literature reveals 25% to 36% of biopsies for calcifications are malignant. Thus, calcifications are sensitive but not specific markers of breast cancer. A novel method has been developed to allow mammographic differential diagnosis based upon the 3-D orientation and morphology of breast calcifications. With this method, image reconstruction can be performed reproducibly. Biopsy specimens and *in vivo* calcifications have been examined. In instances where calcifications are associated with a mass, one can distinguish preferentially peripherally distributed calcifications from homogeneously distributed calcifications. It is also possible to elucidate the linear distribution of calcifications contained within a ductal system. This research study was specifically aimed at advancing the methodology of image reconstruction, and validating the technique with a small clinical trial.

2. Report Body

2.1. Background

There is evidence that both the mortality and morbidity resulting from breast cancer can be reduced with early detection.[1,2,3,4]. While many imaging modalities have been investigated for the diagnosis of breast cancer, film-screen mammography is currently the most sensitive modality available for the early detection of this disease[5,6,7,8]. In current clinical practice, both symptomatic and asymptomatic women have a two view mammographic examination consisting of medio-lateral and cranio-caudad film images of each breast. If there is cause for suspicion, then additional film images are obtained, including "cone-down views" in which extra compression is applied to the suspicious region of the breast to obtain an image with less overlaying tissue, and "magnification views" in which the geometry of image acquisition is altered to magnify the suspicious region (increasing the image signal-to-noise ratio at the expense of dose). In spite of these additional procedures, such approaches often fail to clearly indicate or contraindicate malignancy. As a result, a large number of benign biopsies are performed. Approximately 1 in 4 biopsies will result in the detection of a cancer.[9] Benign biopsies represent a major expense and one of the largest deterrents to women entering a screening mammography program. A definitive, non-invasive method of distinguishing between benign and malignant breast lesions is essential.

The detection and differential diagnosis of subtle lesions using film-screen mammography is further hindered by technical limitations, including insufficient film latitude, film granularity noise, and dose-inefficient scatter rejection.[10] These technical limitations arise in part because the film serves as the detector, the image display device, and the image storage device. These limitations can be overcome with a digital imaging system, because the processes of acquisition, display and storage are performed independently and can be optimized separately.[11] Digital mammography is likely to lead to other improvements in diagnostic and screening mammography. The digital format and higher image quality are well suited to computer-aided diagnosis, digital image processing to optimized lesion conspicuity, and allows advanced imaging techniques such as 3D imaging, dual-energy imaging, and contrast-enhanced mammography. In this grant, we investigated a novel technique for performing 3D imaging of breast calcifications using a low-dose technique known as limited-view tomography (LVT). We believe that such advanced techniques may provide a method by which to reduce the necessity of breast biopsies.

It has been reported that 29% to 48% of nonpalpable carcinomas are visible on the basis of calcifications alone.[9,12,13,14,15,16] Calcifications are especially important as a sign of early breast cancer.[9,17,18] Although certain calcifications are pathognomonic of malignant or benign lesions, so that biopsy is definitely indicated or contraindicated, in other instances the appearance is indeterminate, suggesting the possibility of carcinoma to varying degrees. A review of the literature reveals 25% to 36% of biopsies for calcifications are malignant.[14,19,20,21,22,23] Thus, calcifications are sensitive but not specific markers of breast cancer.

In a seminal work[24], Lanyi has shown that the determination of malignancy in mammography has failed, in part, due to the processes of projection and superimposition that occur when any 2-D image is produced of a 3-D object. The result is a loss of information regarding the structure and morphology of breast lesions. In 1988, Lanyi[24] advocated a 3-D morphologic analysis of breast calcifications to overcome these limitations and demonstrated the utility of this approach using a technique that required biopsy. We took heed of Dr. Lanyi's hypothesis and developed, as part of this grant, a method for imaging calcifications in 3-D based upon LVT[25,26,27,28,29]. In this report, we describe the final results of a clinical trial of the LVT imaging technique.

2.2. Summary of Hypothesis and Specific Aims

In the original grant application, three hypotheses were stated. These hypotheses were to be tested as follows:

1. A comparison of the positive predictive value of film-screen mammography (FSM) and 2D digital mammography (2DM).
2. A comparison of the positive predictive value of FSM and 2DM vs. 3D digital mammography.
3. Correlation of the 2DM and 3DM characteristics with the histologic appearance to provide new criteria to differentiate breast calcifications associated with benign and malignant histology.

These tests were translated into the following five specific aims:

1. Test whether FSM/2DM is more accurate than FSM alone for the evaluation of breast calcifications.
2. Test whether FSM/2DM/3DM is more accurate than FSM/2DM.
3. Compare the cost effectiveness of using FSM/2DM and FSM/2DM/3DM in the analysis of false-positive biopsies for calcifications.
4. To test inter-reader variability of 2DM and 3DM.
5. To provide new imaging criteria to differentiate between benign and malignant calcifications based on 2DM and 3DM correlation with breast histology.

2.3. Timeline and History

It is useful to discuss the timeline and events that have shaped the life of this research project. When first proposed, the work was to be performed by Emily Conant (PI and lead radiologist), Andrew Maidment (co-investigator), Anna Vincente (radiologic technologist) and Michael Albert (research assistant). Two additional radiologists were to act as readers. The grant began August 15, 1996. However, in August 1997, Dr. Conant left Thomas Jefferson University. At that time, work on the grant stopped. It was not until May 20, 1998 that the contract was revised, and Dr. Maidment was officially appointed as the PI of the grant.

Since the departure of Dr. Conant, there have been a number of additional people start and leave the TJUH breast center, including Dr. Stephen Feig, Dr. Dionne Farria, Dr. Jane Hughes, Dr. Stephen Nussbaum, Dr. Stephen Lee, Dr. Barbara Cavanough, and

others. This has had a significant negative impact on all of the research being performed at the breast center. In 1999, the Fischer Mammotest imaging system that was used in this grant was sold by the hospital. This last act definitively ended patient accrual. Finally, due to a dramatic increase in clinical responsibilities, Dr. Maidment and Dr. Albert were not able to allocate much time to this project between 1998 and 2000. Several no-cost grant extensions were requested and approved by the DOD during that time.

In spite of these problems, some significant research has come out of this grant, particularly in advancing the LVT image acquisition and display techniques. At the same time, the clinical trial has been less successful. Contrary to previous studies,[26,27,28,29] 2D and 3D digital mammography did not show an appreciable benefit over film-screen mammography. Potential reasons for this discrepancy, and a series of "lessons learned" are summarized in section 2.11.

The work on this grant is presented in eight parts: image acquisition methodology, image reconstruction technique, image display methodology, evaluation of the image reconstruction methodology, the clinical trial design, a description of the patient population, the clinical trial results, and a discussion.

2.4. Image Acquisition

3-D images of calcifications are reconstructed from digital mammograms acquired on a prone stereotactic breast biopsy system (Fischer MammoTest™, Denver, CO). The biopsy system is fitted with a small field-of-view digital mammography detector (Fischer MammoVision™) that produces images that have a format of 1024 x 1024 pixels. Each pixel has a size of 48 μm, and is digitized as a 12-bit value. Images are acquired at the Thomas Jefferson University Breast Imaging Center. The images are then transferred to the University's Radiological Imaging Research Laboratory via ethernet using FTP.

The image acquisition geometry is illustrated in Figure 1, where an object (x,y,z) is shown being imaged with the x-ray tube at point Q_1, yielding a projection at (u_1,v). Similarly, when the x-ray tube is at point Q_2, the object is projected to (u_2,v). A simple transformation from (u_1,u_2,v) to (x,y,z) is required to determine the 3-D location of the object. In routine usage of the biopsy system only 3 images are acquired (-15°, 0° and +15° relative to the perpendicular vector to the detector). However, as discussed in Section 2.7, a larger number of views may be acquired to improve the reconstructions. We have examined reconstructions that have used up to seven views of the breast, acquired in 15° increments from -45° to +45° (a total of 90° apart). A trade-off exists between the number of views and the dose incurred in the study. It is for this reason that CT of the breast is not performed.

The mean glandular dose in the 3-D imaging procedure is similar to an average 2 view per breast mammography examination (2.5 mGy), and typically is less than is used in a magnification image of the breast. Each digital projection image of the breast is performed at a mean glandular dose of approximately 0.6 mGy. Thus the total mean

glandular dose required to perform a 3-D study is between 1.8 mGy and 4.2 mGy, depending upon the number of views acquired.

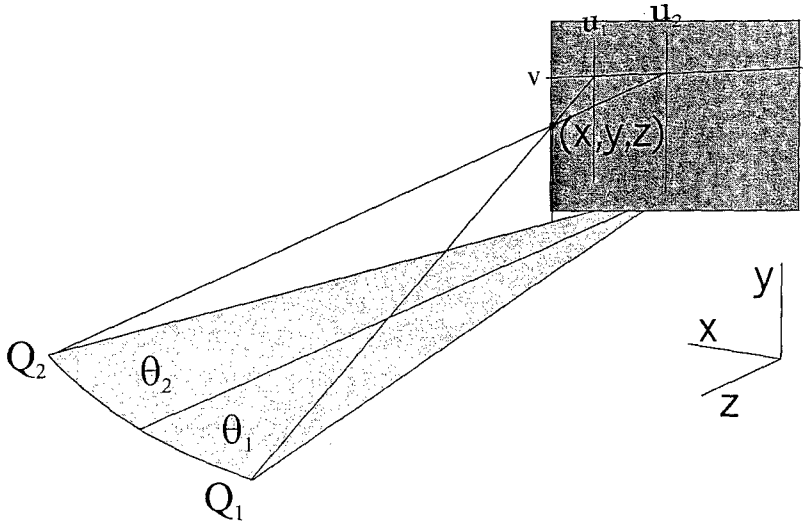

Figure 1: Schematic of the image acquisition geometry.

2.5. Image Reconstruction

Image reconstruction follows in 3 steps. First, candidate calcifications must be found and segmented from the background of the image. Second, the candidate calcifications must be matched between the two or three views used in the reconstruction, and any motion between the views must be determined. Finally, the 3D location and shape of each calcification is determined by limited-view tomography (LVT).

2.5.1. Identification of Calcification Candidates

Currently, the calcifications in each image are identified manually. In this process, a seed point is placed near the center of a calcification by a human operator. The calcification is then segmented semi-automatically using a recursive region-growing algorithm. Next, the corresponding projected image of the calcification is identified in the second view, and the calcification is segmented. These steps are repeated for every calcification for which correspondence between the views is found.

The segmentation algorithm assumes that the seed point is located near the center of the calcification. Any pixel adjacent to the seed point with a digital value significantly below the local average is added to the segmented region, and pixels adjacent to these pixels are in turn tested. The local average is calculated as the mean signal intensity of the 50x50 pixel region centered on the seed point, and pixels are considered to be significantly below the average if they are less than the average by more than four times the local noise. This local noise is computed by dividing the 50x50 pixel region into 4x4 sub-regions, calculating the RMS value in each sub-region, then taking the median of the RMS values. Next, a "background region" surrounding each calcification is calculated. This region is used to estimate the intensity of the signal that would occur in the absence of calcific material at each pixel in the segmented calcification. This signal is denoted

I_{bg}. The attenuation due to calcium can then be calculated as $I_{ca} = I_{bg} - I_{obs}$, where I_{obs} is the observed intensity of the signal in the calcific pixel prior to subtraction.

2.5.2. Matching Calcifications between Views

It is possible to correlate the projected image of each calcification in the different views of the breast from the positions, shapes and sizes of the projected images. Note, for example, that the two projected positions [(u_1, v) and (u_2, v)] of a calcification at position (x,y,z) share a common coordinate, v, as shown in Figure 1. It is possible, therefore, to use the mass of the calcifications that span a similar range of v values to determine which projected shadow corresponds to which calcification in each view. By adding additional views, one can then verify the calculated 3-D position against the segmented calcifications in those views, as well as identifying those calcifications that are hidden or obscured in one or more of the other views. In this manner, it is possible to identify each calcification in each view. For this study, the matching between views was performed manually by a skilled technician.

2.5.3. 3D Limited-View Tomography

Once x-ray shadows of corresponding calcifications are identified in all projections and the geometric acquisition parameters were adjusted to compensate for motion or uncertainties in the geometry, the three dimensional geometric shape of the calcifications is estimated by a binary reconstruction. The binary reconstruction is performed using a three dimensional array of volume elements centered at the reconstructed position of the calcification. The array is of 100x100x100 volume elements, each element being 48 μm on the edge to match the size of the detector elements.

Reconstruction was attempted in one of two ways. If more than two projections were available, a simulated annealing application was applied. Otherwise, the reconstruction was approached in a heuristic fashion comprising three steps:

1. A preliminary estimate based on consistency with all of the projected shadows.
2. Trimming of the long tails in the direction perpendicular to imaging plane.
3. Morphological smoothing.

2.5.3.1. Heuristic Algorithm

Step 1: For each volume element, the projection of the center of the volume element into the imaging plane was calculated. If the projected point was inside the segmented shadow of the calcification in each view, the volume element was tentatively identified as being filled with calcified material and inside the calcification, and was so labeled. Any adjacent volume elements were labeled as volume elements that could become part of the calcification upon further processing. Thus, the region into which the reconstruction could extend was a 1-fold dilation of the preliminary estimate.

Step 2: As the angles at which the projection images were acquired covered a relatively narrow range, it was found that the preliminary estimate made in step 1 showed an obvious artifact in that the candidate reconstructed volume was elongated in the direction

perpendicular to the imaging plane (the z-direction). To compensate for this, in each horizontal (y) plane, the smallest rectangle constraining all volume elements was identified as being in the calcification by step 1 with sides parallel to the x and z directions. From the center of this rectangle, a circle was constructed whose radius was 10% greater that one-half the average of the lengths of the sides of the rectangle. All volume elements in the plane not lying in the circle were then removed from the preliminary estimate of the volume reconstruction.

Step 3: The morphological smoothing consists of a morphologic shrinking operation followed by a dilation. For the shrinking, any volume element of which one of the six immediate neighbors is not in the reconstructed volume is removed from the reconstructed volume. For the dilation, any volume element of which one of its six immediate neighbors is still in the reconstructed volume after the shrinking is added to the reconstructed volume.

2.5.3.2. Simulated Annealing

When multiple views are available, we can apply the simulated annealing algorithm show in Figure 2. Every possible shape of the calcification is associated an "energy" function of the form

$$\chi^2 = \sum \left(t_{calc} - \ln\left(I_{bg} / I_{obs} \right) \right)^2 \qquad (1)$$

which measures how poorly the given shape reproduces the observed shadows. Here I_{obs} represents the digital value measured in a pixel, I_{bg} is the estimated value which would have been observed at that position in the absence of the calcification, t_{calc} is the length of intersection of the calcification with the line running from the x-ray source to the pixel, and the sum is taken over all points in the 50 x 50 pixel region. In order to estimate I_{bg} for pixels in the calcification, a linear fit is made to the digital values in a ring of pixels between 3 and 6 pixels away from the boundary of the calcification. Outside the calcification $\ln(I_{bg}/I_{obs}) = 0$ by definition. In these calculations the effective attenuation length of the material constituting the calcification is taken as a parameter to be fitted to account for the varying consistencies of the calcific materials, the effects of beam hardening through different thicknesses of tissue in the different views, and the effect of scatter.

The mask computed above is used as the starting configuration for a simulated annealing process. At each step of this process a voxel is randomly chosen such that, if it is in the calcification, it has at least one neighbor outside the calcification, and if it is outside the calcification, it has at least one neighbor inside. The effect on the energy function, $\delta\chi^2$, of changing the state of the chosen calcification is then computed. The probability of the change actually occurring is given by

$$e^{-\left(\delta\chi^2/kT\right)} \qquad (2)$$

where kT is a unitless quantity which represents the effective temperature at each stage of the annealing process. Thus, initially the search explores a wide range of configurations, most of which do not fit the data well. As the process continues, the effective temperature is reduces and the search is restricted to a smaller region of the relevant phase space. In this manner, a 3-D reconstruction of each calcification is made.

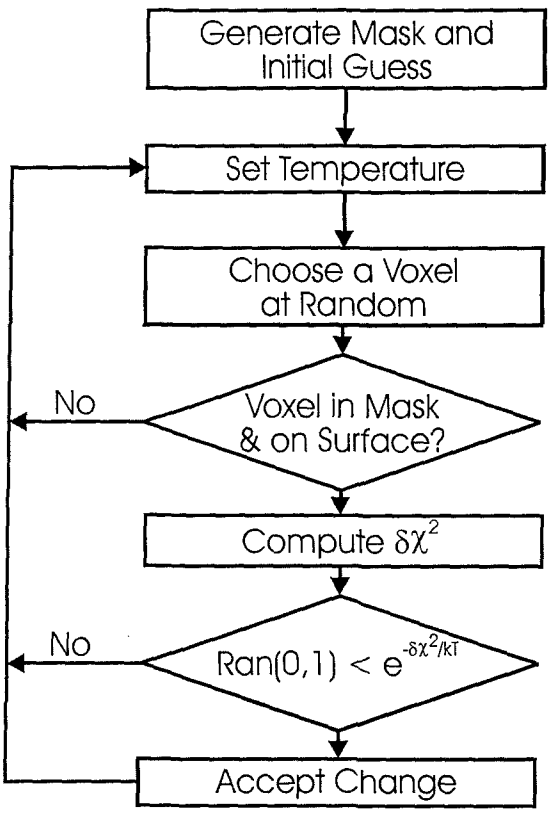

Figure 2: Flowchart of the simulated annealing process

2.6. Image Display

The resulting reconstructions were displayed using the OpenGL[3031] extension to X-Windows on a Sun workstation. Each reconstructed volume, consisting of a distinguished set of cubic volume elements, was used to generate a surface via the marching cubes algorithm[32]. The illumination of the resulting surfaces was performed with a combination of diffuse lighting and a virtual directional light source positioned in front of the monitor and to one side. The calcification cluster was scaled to efficiently use the monitor. Controls were provided to allow the user to rotate the model cluster.

Stereoscopic display was performed using OpenGL to render the left-eye and right-eye perspectives into a pair of stereo buffers window under the X-windows stereo extension. The monitors used were capable of displaying 960x680 pixels at a refresh rate of 112 Hz, so that no flicker was observed when the stereo images where viewed through a liquid crystal shuttering system synchronized with the display. The disparity between the two images was adjusted so that the geometric center of the cluster would appear at the center of the screen and at the same depth as the screen. The disparity between views was

adjusted so that the distances in the displayed cluster were proportional to distances in the reconstruction. This proportionality is only approximate, as the display does not compensate for head motion.

The reconstructed calcifications could be viewed as either wire-frame images or as surface rendered images. Viewers could also choose between stereoscopic and monoscopic display. Anecdotally, radiologists generally preferred to look at surface rendered images, often looking at both the stereoscopic and monoscopic display.

2.7. Evaluation of Reconstruction Methodology

An example of the results of the simulated annealing algorithm is show in Figure 3. In computing this example, a 400 μm diameter sphere with a large cavity was simulated and additively superimposed upon experimentally acquired digital images of a uniform Lucite test phantom. Images of the phantom were acquired at angle between -45° and 45°, in 15° increments. Images of the object were simulated at the same angles. X-ray quantum noise was evident in the images and was maintained in simulated images of the object. The cavity was oriented away from the x-ray tube 0° position, thus the 2-D images of the object appear disk-like. The simulated calcification is shown from several perspectives in the first column of Figure 3. The following columns show the results of reconstruction by simulated annealing using information from 3, 5, and 7 views, viewed from the same perspectives. In all cases, the reconstruction shows an object that is round with a distinct depression on the same side as the simulated calcification, so that the morphology of the calcification is preserved in the reconstruction. As the number of views increases this shape becomes qualitatively clearer. For the 7-view reconstruction, the overlap between the reconstructed volume and the volume of the simulated calcification is 90% of the volume of the calcification. The discrepancy consists almost entirely of voxels on the surface of the calcification. Given the pixel size of the detector, the error in the position of the boundary cannot be smaller that ~25 μm. For a 200 μm radius sphere, a 25 μm skin accounts for 30% of the volume, so surface voxels affect the overlap volume significantly more than might be expected. These voxels do not, however, impede the ability to identify this object as having a cavity that would not be evident when viewing the 2-D images.

2.8. Clinical Trial Design

The clinical trial was original designed to obtain FSM, 2DM and 3DM images from 100 women undergoing breast biopsy indicated by breast calcifications. We were able to obtain image data on 130 women from two different methods. Both study methods were conducted under IRB review. The first (TJU IRB control #93.0705) consisted of a retrospective review of images from 74 patients who had had a stereotactic core biopsy for breast calcifications, or of breast tissue specimens containing calcifications. In the latter case, the specimens had been imaged in a water bath to simulate breast tissue of equal thickness to a normal breast. However, as we shall discuss below, these latter images lack the complexity of background structures that are found in real mammograms, and were excluded from the reader study. The second study (TJU IRB control #96.0160) was a prospective study of women having core breast biopsies, for which 56 women were recruited.

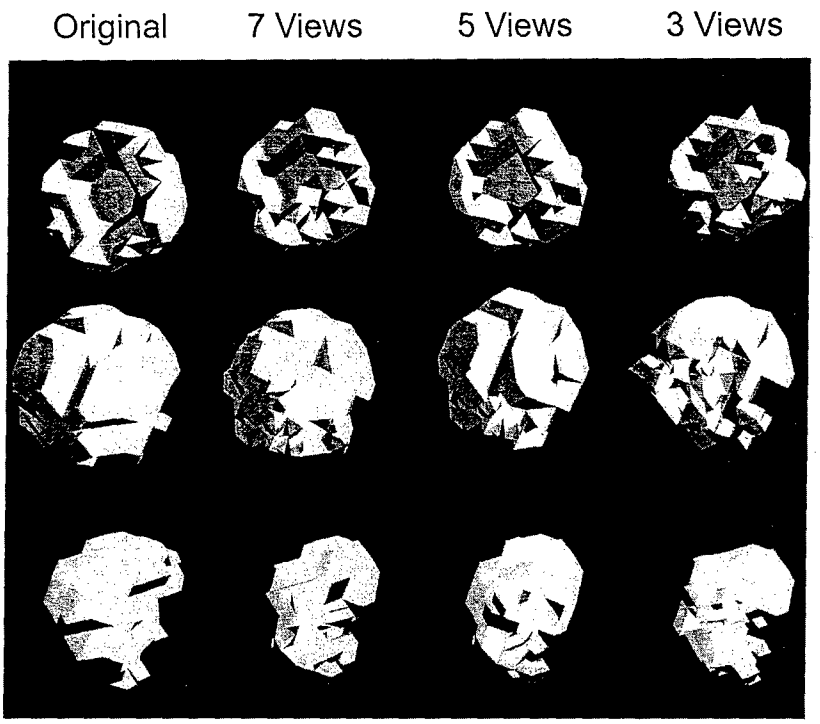

Figure 3: 3 reconstructions of a simulated calcification, showing the original and three reconstructions made using simulated annealing from 3, 5 and 7 views of the object.

For each patient or specimen in the study set, three images of the breast were obtained at ±15° of separation, and 3DM images were produced, as described in sections 2.4 and 2.5. 2DM and 3DM images were digitally archived for use in the study. FSM images were maintained in the Jefferson radiology film library. At all times, patient confidentiality was maintained.

Three readers participated in the study. Each was a highly trained academic radiologist, who subspecializes in mammography. The readers were given training sessions, followed by 2 to 4 reading sessions. Each reading session took 1 to 2 hours.

The radiologists were presented with a set of case, randomly ordered. Images from each case were presented in the same order – FSM first, 2DM second, and 3DM last. After examination of a case in each modality, the reader was asked to rate the likelihood of malignancy on a continuous scale from "benign" to "malignant", by making a mark on a line (see Figure 4). They were also asked to mark whether they would biopsy the case or not based upon their cumulative experience from reading each modality in turn. Finally, they were asked to comment upon the findings in each case.

There was considerable debate when the scoring system was written. Some readers wanted a 5-point scale, while others preferred the continuous scale. Other arguments centered on the wording of the question(s) to be asked. Radiologists do not judge malignancy, only the suspicion of malignancy. The latter working was used to instruct the radiologists. Other possible questions included "confidence that the person should go for biopsy." However, the radiologists in question felt that this was a binary scale. The

language for "BX (biopsy): Yes/No" arose from this discussion. It also allowed us to determine if the linear scale was being used consistently.

The FSM images were presented on a standard mammographic viewbox. The readers were allowed to see all pertinent film-screen mammograms, including the 4 canonical views and any magnification or spot compression views. Additionally, ultrasound was shown where available. The radiologists had a magnifying glass available to them as well.

The 2DM images were presented on a computer monitor. The radiologists had the ability to manipulate images at will. The radiologists could window and level, magnify and invert the grayscale. The 3DM images were presented on a computer workstation as described in section 2.6. Controls were provided to allow the reader to rotate the calcification cluster in 3D, continuous spin the object in arbitrary directions, and view the object as surface rendered or as wire frame models. The objects could be viewed either monoscopically or stereoscopically. Typically, readers only viewed the object surface rendered with stereoscopy enabled.

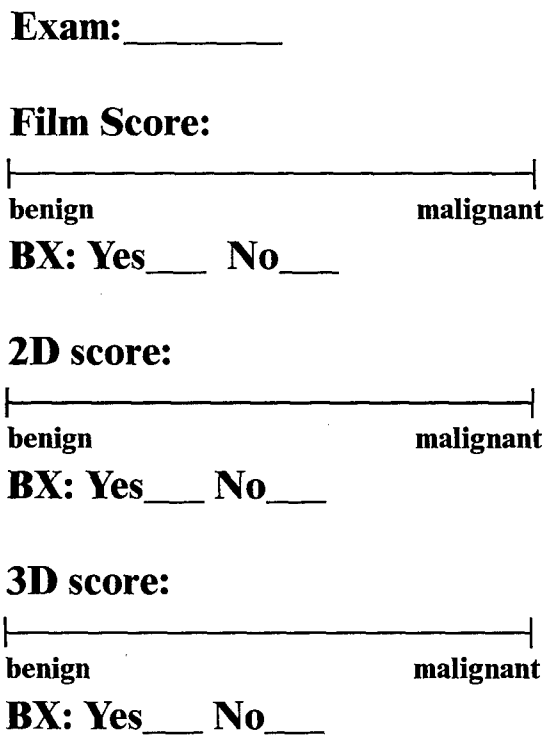

Figure 4: Score sheet used by radiologists to evaluate each case.

2.9. Patient Population

In total, 130 cases where acquired and entered into the database. Of the 130 patients in the database, 120 were full *in vivo* 2DM and 3DM clinical studies. The remaining 10 were cases in which specimens were imaged *ex vivo*. Of the 130 cases, 42 were malignant (32.3%). A summary of patient ethnicity is given in Table 1. The racial distribution is similar to our patient population as a whole.

IRB Control #	White	Black	Asian/ Oriental	Other	Unknown	Total
93.0705	59	11		1	3	74
96.0160	43	6	1		6	56
Total	102	17	1	1	9	130

Table 1: Summary of Patient Race of the Image Database

Of the 126 eligible patients, 40 (31.7%) had cancer, 86 (68.3%) did not. An equal number of biopsies were performed on the left and right breast (63 each). The distribution of malignant and benign cases was also equally divided between the left and right breasts (20 each for malignant cases, and 43 each for benign cases). The ages of the patients is shown in Figure 5. There is insufficient numbers to definitely discern a difference in the age distributions of patients with benign and malignant biopsy findings, however, it appears that malignancies were most common in the 50-59 year olds, due to the large number of such women.

The results of pathology are shown in Table 2. The ductal carcinoma sub-type was often unspecified, but specified subtypes included solid, comedo, papillary and micro-papillary. The case of Paget's disease was associated with a ductal carcinoma. The number of entries does not sum to 130, as some women had multiple findings, while others had none.

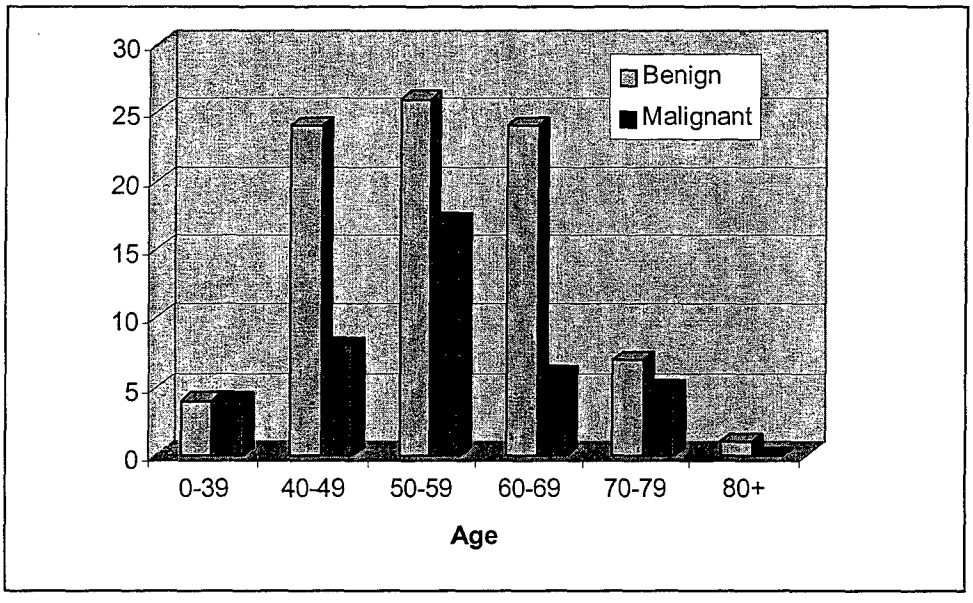

Figure 5: Age Distribution of Patients

Malignant		Benign	
Ductal carcinoma	25	Fibrocystic change	48
Ductal carcinoma *in situ*	23	Ductal hyperplasia	29
Lobular carcinoma *in situ*	2	Fibroadenoma	22
Papillary neoplasm	1	Sclerosing adenosis	16
Paget's disease	1	Fat necrosis	3
		Duct ectasia	2
		Lobular hyperplasia	2
		Papilloma	2
		Radiation induced changes	2

Table 2: Summary of Pathology Results

Of the 130 patients, 42 were selected for the reader study. Many of the 130 cases did not have complete films to allow a full comparison. In addition, as mentioned above, 10 studies were of biopsy specimens. These were not included in the reader study, as they lack sufficient background detail and more clearly portrayed the calcifications than did in FSM images. Of the 42 cases in the reader study, 14 were malignant and 28 were benign (33.3% and 66.7% respectively). Lesions were almost equally distributed between the right (22) and left (20) breasts. The age distribution of the reader study set is shown in Figure 6.

The numbers of calcifications that were included in the 3D images are shown in Figures 7 and 8. Figure 7 addresses those cases, excluding specimens that were imaged in 3D. Figure 8, includes only those cases used in the reader trial. There are fewer calcifications in the malignant cases; however, the small number of cases limits the generality of this statement.

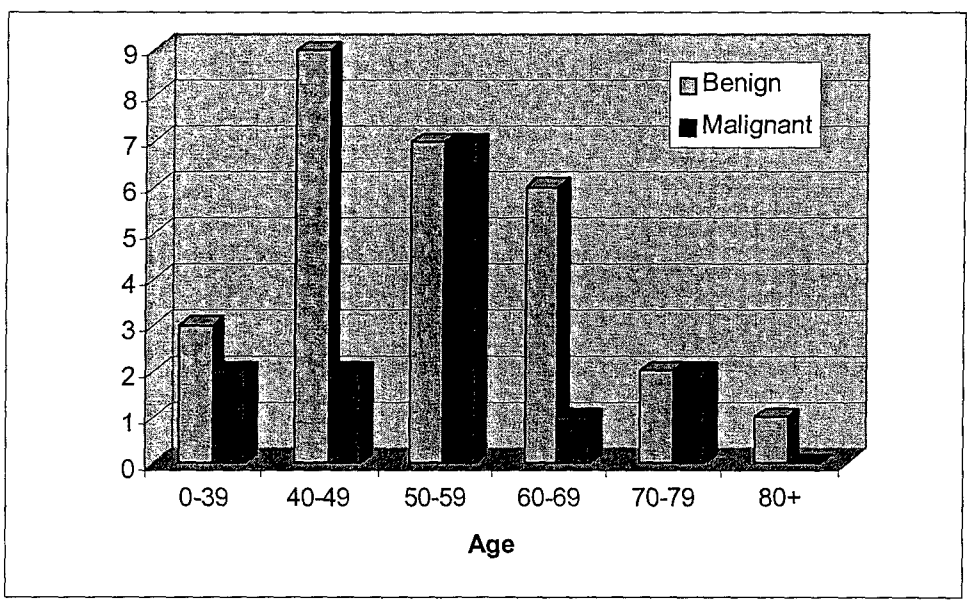

Figure 6: Age Distribution of the 42 patients included in the reader study.

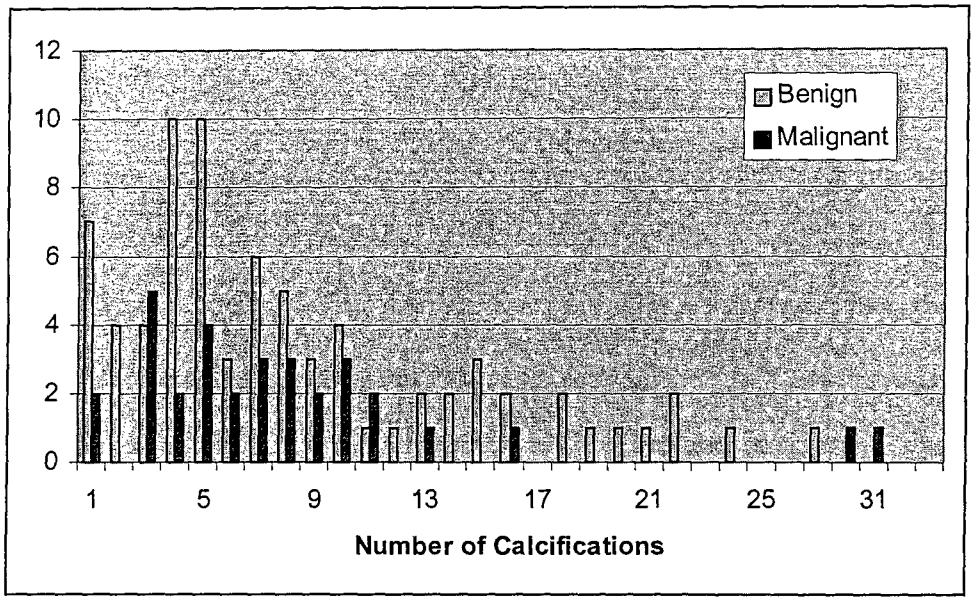

Figure 7: Histogram of the number of calcifications which could be matched between views for 110 cases prepared in 3D

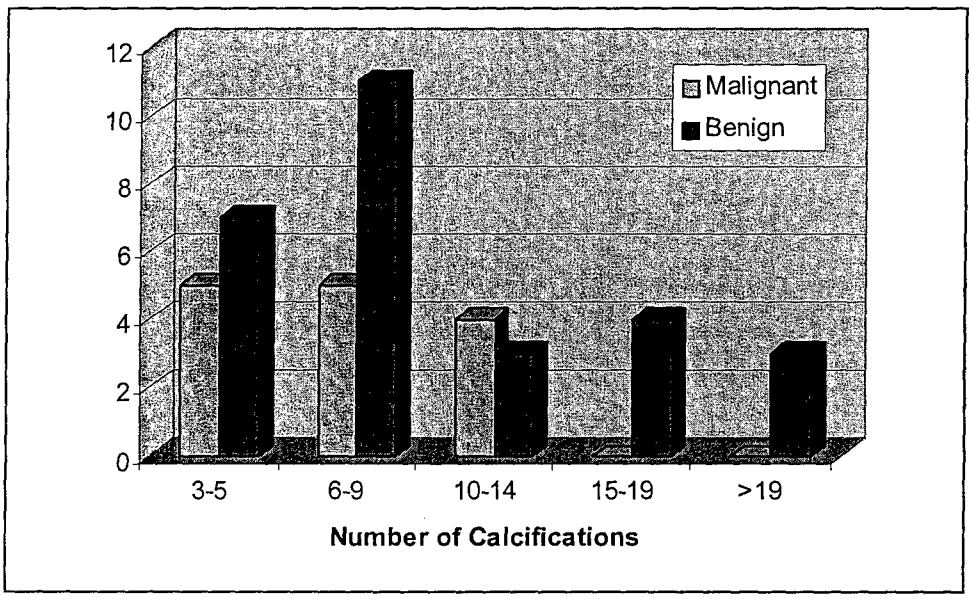

Figure 8: Histogram of the number of calcifications, separated into malignant and benign cases.

A number of other aspects of the calcifications were examined, including calcification size (volume), their shape, etc. No readily discernable trends were evidence. However, as explained in section 2.10 the radiologists were able to discern certain features of calcification clusters, which were felt to be clinically relevant.

2.10. Clinical Trial Results

2.10.1. Biopsy Recommendations

Part of the clinical trial involved a determination of the need for a biopsy. After viewing each case in each mode (cumulatively), the readers were asked to rate the need for biopsy. As this was a binary rating, it was possible to compute various metrics shown in Table 3.

	% TP		
	FSM	2DM	3DM
R1	100.0%	92.3%	92.3%
R2	100.0%	100.0%	100.0%
R3	100.0%	100.0%	92.3%

	% TN		
	FSM	2DM	3DM
R1	17.2%	17.2%	20.7%
R2	32.1%	35.7%	35.7%
R3	0.0%	7.7%	18.5%

	% Correct		
	FSM	2DM	3DM
R1	42.9%	40.5%	42.9%
R2	52.5%	55.0%	55.0%
R3	32.5%	38.5%	42.5%

	PPV		
	FSM	2DM	3DM
R1	35.1%	33.3%	34.3%
R2	38.7%	40.0%	40.0%
R3	32.5%	35.1%	35.3%

	NPV		
	FSM	2DM	3DM
R1	100.0%	83.3%	85.7%
R2	100.0%	100.0%	100.0%
R3	n/a	100.0%	83.3%

Table 3: The true positive (TP) fraction and true negative fraction (TN) expressed in percent, the percent correct for all cases ((TP+TN)/number of cases), as well as the positive predictive value (PPV) and negative predictive value (NPV). (n/a – all benign cases recommended for biopsy).

With one exception, use of 2DM and 3DM images did not significantly alter observer performance. Reader 3 did shown improved specificity with 2DM and 3DM. In the case of film, Reader 3 felt all cases required biopsy, however, with the inclusion of 2DM and 3DM, the number of negative biopsy recommendations dropped by 2 and 5 respectively. These differences were not statistically significant.

2.10.2. ROC Analyses

The continuous suspicion of malignancy scale readings were converted into values between 0 and 1, by measuring the location where the marking crossed the line on the scale. These data were used to calculate the area under the ROC curve, A_z. These data are shown in Tables 4 and 5. Table 4 was calculated using the simple Wilcoxan method, while Table 5 was calculated by fitting to a binormal distribution, following the work for multi-reader, multi-case (MRMC) observer studies by Dorfmann, Berbaum and Metz.[33] The graphs of ROC performance are shown in Figure 9.

The ROC data do not show a statistically significant difference in observer performance between FSM, 2DM and 3DM. This is contrary to our pilot data.[26,27] There was a statistically significant difference in performance between Reader 1, and Readers 2 and 3. It is important to note that the performance of Reader 1 is significantly less than the other two readers ($p < 0.05$). The result for Reader 1 for 3DM is no better than random guessing. This will be discussed in detail in section 2.11

Additional evaluations of ROC using various subsampling strategies were attempted, but these attempts did not elucidate the problems with the reader study.

Reader	FSM	2DM	3DM
R1	0.6324+-0.0999	0.6220+-0.1003	0.4539+-0.0991
R2	0.8199+-0.0808	0.7917+-0.0853	0.7321+-0.0927
R3	0.8497+-0.0751	0.8214+-0.0806	0.7649+-0.0890

Table 4: A_z calculated using the Wilcoxan method.

Reader	FSM	2DM	3DM
R1	0.6393+-0.0908	0.6264+-0.1069	0.4868+-0.1061
R2	0.8283+-0.0678	0.7939+-0.0709	0.7443+-0.0758
R3	0.8585+-0.0702	0.8365+-0.0749	0.7787+-0.0832

Table 5: A_z calculated using the MRMC method of Dorfmann, Berbaum and Metz.

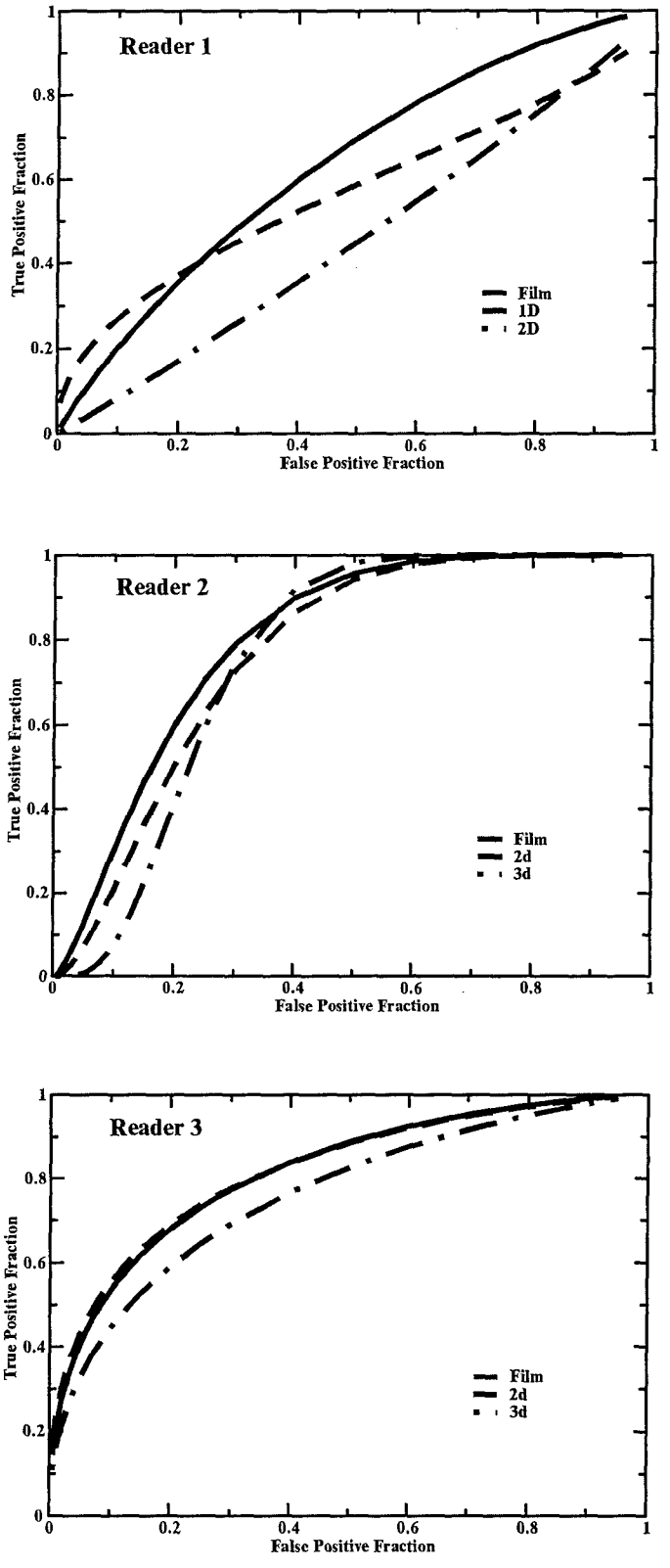

Figure 9: ROC performance for the three observers, calculated using the MRMC method of Dorfmann, Berbaum and Metz

One of the reasons that a binary "biopsy"/"no biopsy" question was included in the study, was to determine the efficacy of use of the continuous "suspicion of malignancy" score. In theory, the responses for the benign and malignant cases should have formed a continuum between 0 and 1. As shown in Figure 10, this was the case. However, one would also expect that the threshold between "no biopsy" and "biopsy" would have been fixed, and that the highest score of "no biopsy" cases would have been lower than the lowest score of a "biopsy" case. This was not observed for Reader 1, particularly for 3DM.

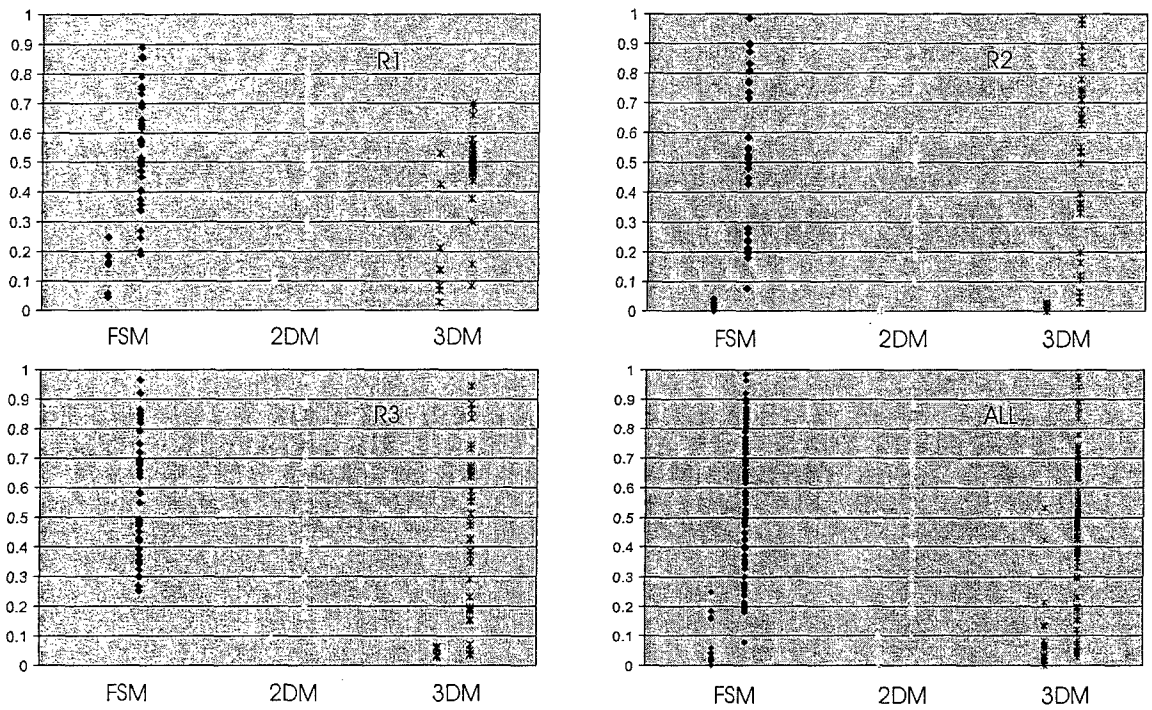

Figure 10: A summary of scores aggregated into BX- (left) and BX- (right) for each of FSM, 2DM and 3DM demonstrating the inconsistent use of the degree of suspicion score.

2.10.3. Descriptive Assessment

As in prior work, we had confirmation of two "features" visible with 3DM. First, In instances where calcifications are associated with a mass, we could distinguish preferentially peripherally distributed calcifications from homogeneously distributed calcifications. The former are almost universally associated with benign fibroadenomas, which are calcified (e.g., see Figure 11), while the latter are more commonly associated with malignancy. We were also been able to elucidate the linear distribution of calcifications contained within the ductal system. An example is given in Figure 12.

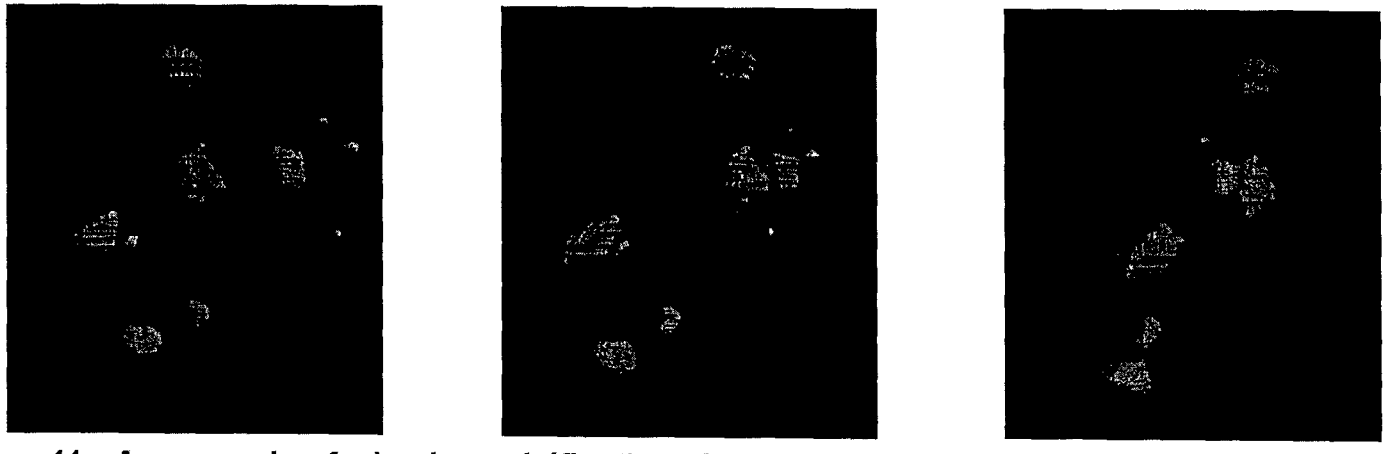

Figure 11: An example of a benign calcification cluster demonstrating a preferentially peripheral distribution, characteristic of a fibroadenoma. The cluster is shown at three different viewing angles.

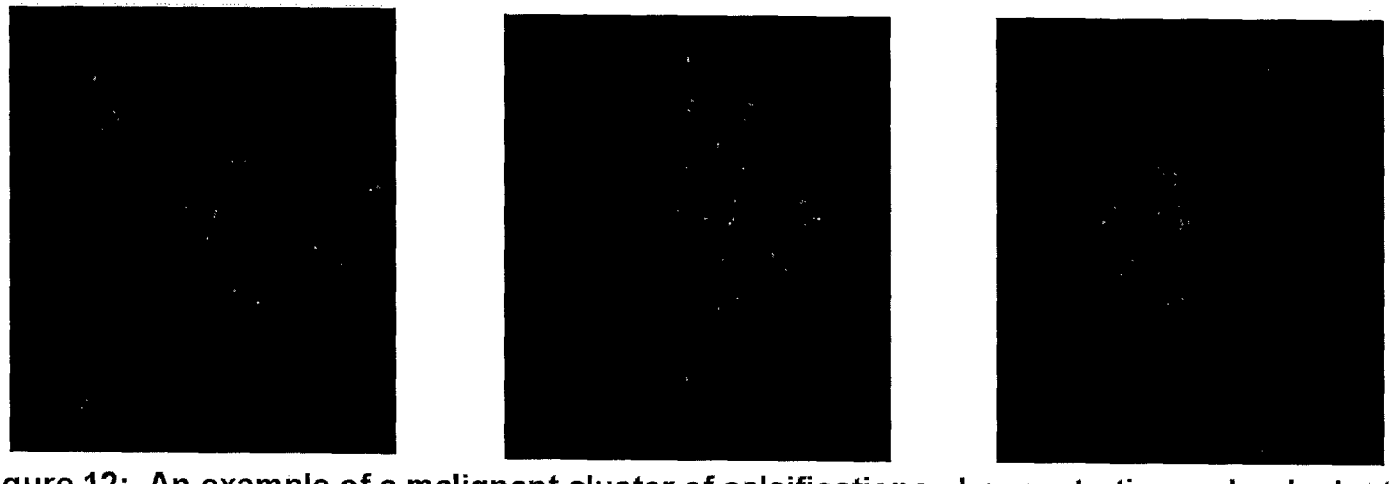

Figure 12: An example of a malignant cluster of calcifications, demonstrating a clearly ductal pattern. The cluster is shown at three different viewing angles.

2.11. Discussion

This project was not an unmitigated success. We were able to continue the development of the techniques needed to provide LVT 3DM images. We have been able to validate these techniques, in part. However, the main goal of the research project was to perform a clinical trial, and we were not able to show any statistically significant benefit to 2DM or 3DM over FSM. This contradicts prior work. In this section, we address some of the limitations of this study and some of the lessons learned.

First, it is now evident that 100 cases are not sufficient. There are many reasons for this. Even if 100 cases are acquired, many film images are removed from the film library over time, so that a retrospective reader study will necessarily involve fewer cases. We cannot copy the films, as the copies have degraded image quality, thus they are neither acceptable for clinical or study use. Moreover, women need their films, and we are mandated to provide them their films under the MQSA act, when they seek referrals or surgical intervention. Thus, even if we image 100 patients, a retrospective study will only allow us to include perhaps ½ of the cases. In hindsight, a prospective study would have been preferable, but certain aspects of the trial, as devised by Dr. Conant, could not be changed later.

The actual study questions, degree of malignancy and need to biopsy, are probably inadequate. However, with the absence of Dr. Conant, there was no single physician advocating this study at Jefferson. While we were able to get three readers, at least one reader (Reader 1), was rushed and distracted throughout the trial. This is evident in her ROC performance, which even for FSM is two standard deviations worse than her colleagues (i.e., Az difference is statistically significant at $p < 0.05$). Moreover, for 3DM, Reader 1 performed at a level consistent with guessing.

The degree of malignancy question seemed to cause consternation to all of the radiologists, particularly Reader 1. She repeatedly expressed her concern with the question because "Radiologist's don't determine malignancy, pathologists do". While this statement is true in and of itself, it belies the role of the radiologist, who must identify as many cancers as possible while recommending as few normal women as possible for biopsy. This question has been used in other clinical trials, both at Jefferson and elsewhere, seemingly without problem. However, this question did not sit well with our particular group of readers.

There are questions as to the suitability of all of the cases included in the trial. A number of cases were excluded from the final clinical trial because we just were not able to segment and match enough calcifications between images. This technique appears to work best when there are many calcifications, or when the specimen is imaged *ex vivo*. The latter finding can be understood by considering the signal-to-noise ratio of the images of specimens. In these instances, we attempted to use a water bath to simulate additional breast tissue, but apparently without success. In would have been better to use Lucite or some other hard, tissue matching material. The result was a higher detector entrance exposure and hence signal-to-noise ratio. In addition, the absence of organized structures superimposed on the calcifications means that the calcifications are more

readily visible in the specimen images. This techniques role in images specimens is an interesting future avenue of research.

Any future test of this methodology requires a better set of metrics for comparing the images, interested and motivated radiologists, careful case selection, and careful image reconstruction. We have addressed the latter issue, in part at least, through developments of a fully automated image reconstruction technique that was developed under a separate DOD grant (DAMD 17-97-1-7143). We have also discovered that it is possible to ascertain the attenuate coefficients of materials with the LVT technique. The value of this discovery is being further investigated in a separate DOD Grant (DAMD 17-00-1-0465).

2.12. Key Research Accomplishments

The following is a list of the key research accomplishments resulting from this work.

- a database of 130 cases of calcifications has been developed
- the methodology for performing limited-view tomography of breast calcifications has been advanced, including improved methods of identifying, segmenting, matching and reconstructing calcifications in 3D.
- software has been developed to implement the algorithms for identifying, segmenting, matching and reconstructing calcifications in 3D.
- software has been developed to display 2DM and 3DM images.
- a clinical trial of LVT 3DM has shown that there is value in better visualizing the morphology of breast calcifications, in terms of descriptive features
- a clinical trial has not shown that there is a statistically significant benefit or detriment to 2DM or LVT 3DM.

3. Reportable Outcomes

3.1. Manuscripts, abstracts, publications

1. A.D.A. Maidment, M. Albert, and E.P. Conant. Three-Dimensional Imaging of Breast Calcifications. In Exploiting New Image Sources and Sensors. Proceedings of the SPIE, 3240, 200-208 (1997)

2. A.D.A. Maidment, M. Albert, E.F. Conant, and S.A. Feig. Three-Dimensional Visualization of Breast Cancer. In Digital Mammography '98, edited by N. Karssemeijer, M. Thijssen, J. Hendricks, and L. van Erning, Kluvier, Holland, 57-60, (1998).

3. A.D.A. Maidment, M. Albert and E.F. Conant. A method for 3-D reconstruction of breast calcifications. Radiology, 201(P), 257 (1996).

4. E.F. Conant, A.D.A. Maidment, M. Albert, C.W. Piccoli, S.A. Nussbaum and P.A. McCue. Small field of view digital imaging of breast calcifications: A method to improve diagnostic specificity. Radiology, 201(P), 369 (1996).

5. E.F. Conant, A.D.A. Maidment, M. Albert, S.A. Feig and P.A. McCue. 2-D and 3-D digital imaging of breast calcifications: A method to improve diagnostic specificity. Radiology, 201(P), 448 (1996).

6. A.D.A. Maidment, M. Albert, E.F. Conant, C.W. Piccoli, and P.A. McCue. Prototype workstation for 3-D diagnosis of breast calcifications. Radiology, 201(P), 556 (1996).

7. A.D.A. Maidment, M. Albert, E.F. Conant, and C.W. Piccoli. A method for three-dimensional imaging of breast calcifications. Medical and Biological Engineering and Computing, 35, Supplement Part 2, 751 (1997).

8. A.D.A. Maidment, M.Albert, E.F. Conant, S.A. Feig, C.W. Piccoli, S.A. Nussbaum, et al. A computer workstation for 3-D imaging of the breast. Radiology, 205(P), 741 (1997).

9. A.D.A. Maidment, and M. Albert, "Automated 3-D Limited-View Binary Reconstruction of Breast Calcifications", CD-ROM Proceedings of the World Congress on Medical Physics and Biomedical Engineering, **4** , July 23-28, 2000.

3.2. Awards

1996 Certificate of Merit, Scientific Exhibit, "2-D and 3-D digital imaging of breast calcifications: A method to improve diagnostic specificity", 82nd Scientific Assembly of the Radiological Society of North America

1997. First Prize, Image Reconstruction and Microscopic Imaging Poster, World Congress on Medical Physics and Biomedical Engineering

3.3. Funding applied for based on this work

1. DOD Breast Cancer Research Grant, DAMD17-97-1-7143. A.D.A. Maidment, PI. "3-D Digital Imaging of Breast Calcifications: Improvements in Image Quality and Development of Automated Reconstruction Methods".

2. DOD Breast Cancer Research Grant, DAMD17-98-1-8169, A.D.A. Maidment, PI. "3-Dimensional Imaging of the Breast".

3. DOD Breast Cancer Research Grant, DAMD17-00-1-0465, A.D.A. Maidment, PI. "A Novel Method for Determining Calcification Compostiion".

4. Conclusions

In summary, we have been able to further develop methods for imaging breast calcifications in 3D. These techniques appear to give value qualitative information about calcification cluster morphology. However, the results of the clinical trial were inconclusive. This is due, in part, to problems encountered in the performance of the trial. In spite of these shortcomings, we expect to be able to publish at least part of this work. Manuscripts for peer-reviewed publications are being prepared currently.

5. References

1 Seidman H *et al.* Survival experience in the Breast Cancer Detection Demonstration Project. *Ca.* **37**:258-290, 1987.

2 Feig SA. Decreased breast cancer mortality through mammographic screening: Results of clinical trials. *Radiology* **167**:659-665, 1988.

3 Shapiro *et al.* Current results of the breast cancer screening randomization trial: The Health Insurance Plan (HIP) of Greater New York, in NE Day and AB Miller (Eds) *Screening for Breast Cancer*, Toronto, Hogreofe, 1988.

4 Tabar L *et al.* Update of the Swedish two-county program for mammographic screening for breast cancer. *Radiol. Clin. N. Am.* **30**:187-210, 1992.

5 Kopans DB *et al.* Breast Imaging. *NEJM* **130**:960-967, 1984.

6 Sickles EA. Breast Imaging: A view from the present to the future. *Diagn. Imag. Clin. Med.* **54**:118-125, 1985.

7 Kopans DB. Non-mammographic breast imaging techniques. *Rad Clin N Am* **25**:961-971, 1987.

8 Kopans DB. Priorities for improved breast cancer imaging, in AG Haus and MJ Yaffe (eds) *Technical aspects of Breast Imaging*, RSNA, Oakbrook IL, 271-274, 1994.

9 Feig SA, Shaber GS, Patchefsky A, *et al.* Analysis of clinically occult and mammographically occult breast tumors. *AJR* 128:403-408, 1977.

10 Nishikawa RM *et al.* Scanned projection digital mammography. *Med Phys* **14**:717-727, 1987.

11 Maidment ADA. *Scanned-slot digital mammography.* PhD. Thesis, University of Toronto, Toronto, Canada, 1993.

12 Wolfe JN. Analysis of 462 breast carcinomas. *AJR* **121**: 846-853, 1974.

13 Frischbier H-J, Lohbeck HU. *Fruhdiagnostik des Mammakarzinoms*. Thieme, Stuttgart, 1977.

14 Bjurstam N. Radiology of the female breast and axilla. *Acta Radiol Suppl* **357, 1978.**

15 Menges V, Busing CM, Hirsch O. *RoFo* **135**:372-378, 1981.

16 Frankl G, Ackerman M. Xeromammography and 1200 breast cancers. *Radiol Clin North Am* **21**:81-91, 1983.

17 Moskowitz M. The predictive value of certain mammographic signs in screening for breast cancer. *Cancer* **51**:1007-1011, 1983.

18 Anderson I. Mammographic screening for breast carcinoma. Ph.D. Thesis , Malmo, 1980.

19 Murphy WA, DeSchryver-Kecskemeti K. Isolated clustered microcalcifications in the breast. *Radiology* **127**: 335-341, 1978.

20 Egan RL, McSweeney MB, Sewell CW. Intramammary calcifications without an associated mass in benign and malignant diseases. *Radiology* **137**:1-7, 1980.

21 Sickles EA. Further experience with microfocal spot magnification mammography in assessment of clustered breast microcalcifications. *Radiology* **137**:9-14, 1980.

22 Muir BB, Lamb J, Anderson TJ, *et al.* Microcalcification and its relationship to cancer of the breast. *Clin Radiol* **34**:193-200, 1983.

23 Sigfusson BF, Andersson I, Aspegren K, *et al.* Clustered breast calcifications. *Acta Radiologica* **24**: 273-281, 1983.

[24] Lanyi M. *Diagnosis and Differential Diagnosis of Breast Calcifications.* Springer-Verlag, New York, 1988.

[25] Robert N, Maidment ADA, and Yaffe MJ. Three-dimensional localization and display of breast microcalcifications. *Proceedings of the annual meeting division of medical and biological physics of the Canadian association of physics.* London Ontario, 1989.

[26] Maidment ADA, Albert M, Conant EF and Feig SA. 3-D Mammary Calcification Reconstruction from a Limited Number of Views. *Proceedings of the SPIE*, **2708**, 378-389, 1996.

[27] Maidment ADA, Conant EF, Feig SA, Piccoli CW and Albert M. Three-dimensional Analysis of Breast Calcifications in *Digital Mammography*, Excerpta Medica ICS-1119, Elsevier Sci., Holland, 245-250, 1996.

[28] A.D.A. Maidment, M. Albert, and E.P. Conant. Three-Dimensional Imaging of Breast Calcifications. In Exploiting New Image Sources and Sensors. Proceedings of the SPIE, 3240, 200-208 (1997)

[29] A.D.A. Maidment, M. Albert, E.F. Conant, and S.A. Feig. Three-Dimensional Visualization of Breast Cancer. In Digital Mammography '98, edited by N. Karssemeijer, M. Thijssen, J. Hendricks, and L. van Erning, Kluvier, Holland, 57-60, (1998).

[30] M. Woo, J. Neider, T. Davis, and D. Shreiner, OpenGL Programming Guide, 3rd ed. (Addison-Wesley, Reading, Massachusetts, 1999).

[31] O. A. R. Board, OpenGL Reference Manual, 2nd ed. (Addison{Wesley Developers Press, Reading, Massachusetts, 1997).

[32] W. E. Lorensen and H. E. Cline, "Marching Cubes: a high resolution 3D surface reconstruction algorithm," Computer Graphics 21, 163{169 (1987).

[33] Dorfman DD, Berbaum KS, Metz CE. Receiver Operating Characteristic Rating Analysis: Generalization to the Population of Readers and Patients with the Jackknife Method. Investigative Radiology 1992;27:723-731.

6. Research Personnel

Andrew D. A. Maidment, Ph.D.	Principle Investigator
Emily F. Conant, M.D.	Former principle investigator. Left Jefferson 1997.
Catherine W. Piccoli, M.D.	Lead Mammographer. Helped with clinical trial design. Acted as reader.
Michael Albert, Ph.D.	Programmer and Research Assistant.
Lisa Fisher, RT	Radiology Technologist. Responsible for patient interview, data collection and image acquisition.
Lisa Sparacino, RT	Radiology Technologist. Responsible for patient interview, data collection and image acquisition.

7. Appendices

Appendix 1: A.D.A. Maidment, M. Albert, and E.P. Conant. Three-Dimensional Imaging of Breast Calcifications. In Exploiting New Image Sources and Sensors. Proceedings of the SPIE, 3240, 200-208 (1997)

Appendix 2: A.D.A. Maidment, M. Albert, E.F. Conant, and S.A. Feig. Three-Dimensional Visualization of Breast Cancer. In Digital Mammography '98, edited by N. Karssemeijer, M. Thijssen, J. Hendricks, and L. van Erning, Kluvier, Holland, 57-60, (1998).

PROCEEDINGS OF SPIE REPRINT

SPIE—The International Society for Optical Engineering

Reprinted from

26th AIPR Workshop

Exploiting New Image Sources and Sensors

15–17 October 1997
Washington, D.C.

Volume 3240

Three-Dimensional Imaging of Breast Calcifications

Andrew D.A. Maidment, Michael Albert, and Emily F. Conant

Thomas Jefferson University, Department of Radiology
111 South 11th Street, Philadelphia, PA 19107

ABSTRACT

Approximately 50% of breast cancers are detected on the basis of calcifications alone. Regrettably, the presence of such calcifications is non-specific; only 30% of biopsies based on suspicious calcifications are malignant. We have investigated three methods (limited view reconstruction (LVR), synthetic tomography and stereoscopy) for three-dimensional imaging and analysis of microcalcifications. Our aim is to increase specificity by more accurately distinguishing between calcifications indicative of benign and malignant breast lesions. We have demonstrated that 3-D imaging of calcifications is possible using an LVR technique that includes semi-automated segmentation, correlation, and reconstruction of the calcifications. A clinical study of the LVR method is ongoing in which 2-D film and digital images are compared to 3-D images. The images are evaluated using a rating of 1 to 5, where 1 = definitely benign, 5 = definitely malignant, and a score of 3 or higher requires biopsy. To date, 3 radiologists have evaluated the images of 44 patients for which biopsy results were available. The use of 2-D and 3-D digital images resulted in doubling the diagnostic accuracy from 36% to 77%. Comparison to other techniques (stereomammography and synthetic tomography) is ongoing. Additionally, a high resolution CT scanner for breast tissue specimens is under construction for comparison of the reconstructed images to a "gold standard."

Keywords: digital mammography, stereomammography, mammary calcifications, image acquisition, image reconstruction, image segmentation, linear tomosynthesis

1. INTRODUCTION

There is evidence that both the mortality and morbidity resulting from breast cancer can be reduced with early detection.[1-4] While many imaging modalities have been investigated for the diagnosis of breast cancer, film-screen mammography is currently the most sensitive modality available for the early detection of this disease.[5-8] In current clinical practice, both symptomatic and asymptomatic women have a two-view mammographic examination consisting of medio-lateral and cranio-caudad film images of each breast. If there is cause for suspicion, then additional film images are obtained, including "cone-down views" in which extra compression is applied to the suspicious region of the breast to obtain an image with less overlaying tissue, and "magnification views" in which the geometry of image acquisition is altered to magnify the suspicious region (increasing the image signal-to-noise ratio at the expense of dose). In spite of these additional procedures, such approaches often fail to clearly indicate or contraindicate malignancy. As a result, a large number of benign biopsies are performed. Approximately 1 in 4 biopsies will result in the detection of a cancer.[9] Benign biopsies represent a major expense and one of the largest deterrents to women entering a screening mammography program. A definitive, non-invasive method of distinguishing between benign and malignant breast lesions is essential.

The detection and differential diagnosis of subtle lesions using film-screen mammography is further hindered by technical limitations, including insufficient film latitude, film granularity noise, and dose-inefficient scatter rejection.[10] These technical limitations arise in part because the film serves as the detector, the image display device, and the image storage device. These limitations can be overcome with a digital imaging system because the processes of acquisition, display and storage are performed independently and can be optimized separately.[11] Unfortunately, full-field digital mammography will not be widely available for several years. Instead, we propose that the most rapid implementation of digital mammography in the clinic can occur as an adjuvant diagnostic tool to film-screen mammography. There are more than 1000 small field-of-view digital mammography imaging systems installed in the United States for use in digital-mammography-guided stereotactic biopsies. We believe that such digital mammographic units provide an enormous,

SPIE Vol. 3240 • 0277-786X/98/$10.00

readily available resource for performing diagnostic "work-ups". Such work-ups could range from the simple use of the digital image receptor for magnified or non-magnified views of suspicious lesions, to 3-D mammography.

It has been reported that 29% to 48% of nonpalpable carcinomas are visible on the basis of calcifications alone.[9,12-16] Calcifications are especially important as a sign of early breast cancer.[9,17,18] Although certain calcifications are pathognomonic of malignant or benign lesions, so that biopsy is definitely indicated or contraindicated, in other instances the appearance is indeterminate, suggesting the possibility of carcinoma to varying degrees. A review of the literature reveals 25% to 36% of biopsies for calcifications are malignant.[14,19-23] Thus, calcifications are sensitive but not specific cancer markers.

In a seminal work[24], Lanyi has shown that the determination of malignancy in mammography has failed, in part, due to the processes of projection and superimposition that occur when any 2-D image is produced of a 3-D object. The result is a loss of information regarding the structure and morphology of breast lesions. In 1988, Lanyi[24] advocated a 3-D morphologic analysis of breast calcifications to overcome these limitations and demonstrated the utility of this approach using a technique that required biopsy. We took heed of Dr. Lanyi's hypothesis and developed a method for imaging calcifications in 3-D (Refs. 25-27). In this paper, we describe two additional methods for imaging the breast in 3-D with particular attention to breast calcifications.

2. METHODOLOGIES FOR 3-D BREAST IMAGING

We have investigated three methods of imaging the breast in 3-D - stereoscopy, limited view reconstruction (LVR) and linear tomosynthesis. The largest overriding concern in acquiring 3-D images of the breast is the dose involved in acquiring the images. The low energies used in mammography, required to obtain adequate subject contrast, result in relatively high exposures (on the order of 1R per image for an average sized breast). This combined with the relatively high sensitivity of breast tissue to radiation ($w_T = 0.05$, Ref. 28), means that mammography is a moderately high dose imaging procedure. To simply increase the number of views of the breast to acquire 3-D images is not an option. Care must be exercised to reduce the exposure for each view when acquiring 3-D images. It is for this reason that computed tomography (CT) of the breast is not considered clinically viable. In the three approaches described below, we shall consider techniques which require an increasing number of constituent images to generate a 3-D image, but in each instance the constituent images can be obtained with progressively lower doses.

2.1. Stereoscopy

Most human observers perceive the world using a stereoscopic vision system. The eyes of the observer are separated by approximately 7 cm, and because of this they record slightly different images. This effect is enhanced when the object being viewed is held closer to the observer. This binocular disparity, incorporated with clues such as shading from different light sources, superposition of structures and *a priori* information concerning the objects allows the observer to determine the position of objects relative to one another in 3-D.

Figure 1: Digital stereotactic imaging system used to acquire the image data for 3-D rendition.

Stereopsis can be simulated when radiographing the breast by acquiring images that are separated by a small angle and then displayed so that each eye views a different image. In our institution, we acquire images separated by angles of 3° to 5°; the optimum angle has yet to be determined. The images are each acquired with a dose that is approximately 1/2 of that used normally. The images are acquired on a prone stereotactic breast biopsy system (Fischer MammoTest™, Denver, CO), fitted with a small field-of-view digital mammography detector (Fischer MammoVision™) that produces images which have a format of 1024 x 1024 pixels (see Fig. 1). Each pixel has a size of 48 mm, and is digitized as a 12 bit value. Images are acquired at the Thomas Jefferson University Breast Imaging Center.

The stereoscopic mages are displayed on a Sun UltraSparc-2 2170, with Creator 3-D graphics. The images are displayed stereoscopically by presenting the data alternately to the left and right eyes of observers wearing synchronized shuttered eyewear (CrystalEyes™, San Rafael, CA) at 112 Hz. Software for image display was written in C and C++ using OpenGL and X Windows.

2.2. Limited View Reconstruction

LVR was proposed by us to generate true 3-D images of breast calcifications, but without the high dose associated with conventional 3-D x-ray techniques such as CT. We still require relatively high dose projection images (comparable to the dose used in non-grid film-screen mammography) to allow detection of the smallest possible calcifications within each projection image, but the technique requires very few images (typically 3, maximum of 7). This technique is possible because the calcifications are reconstructed from segmented image data, and a binary image reconstruction technique is employed.

The 3-D reconstruction of the calcification images is performed in a number of steps, beginning with acquisition of a limited number of projection images of the breast. Next. the calcifications are segmented from the background of breast parenchyma. The shape, size and position of each calcification in each view are used to determine the correspondence of the calcifications between the views. The 3-D location of each calcification is determined geometrically, and the 3-D shape of each calcification is derived using a simulated annealing approach. Finally, the images are rendered in 3-D, and a morphologic analysis and mammographic differential diagnosis is performed.

As with stereoscopy, images are acquired on a prone stereotactic breast biopsy system at the Thomas Jefferson University Breast Imaging Center. The image acquisition geometry is illustrated in Figure 2, where an object (x,y,z) is shown being imaged with the x-ray tube at point Q_1, yielding a projection at (u_1,v). Similarly, when the x-ray tube is at point Q_2, the object is projected to (u_2,v). A simple transformation from (u_1,u_2,v) to (x,y,z) is required to determine the 3-D location of the object. In routine usage of the biopsy system, only 3 images are acquired (-15°, 0° and +15° relative to the perpendicular vector to the detector). In the clinical study discussed in Section 3.2, only two images were used (-15° and +15°). However, a larger number of views may be acquired to improve the reconstruction. We have examined reconstructions which have used up to seven views of the breast, acquired in 15° increments from -45° to +45° (a total of 90° apart). Each digital projection image of the breast is performed at a glandular dose of approximately 0.6 mGy. Thus, the glandular dose required to perform a 3-D study is between 1.8 mGy and 4.2 mGy, depending upon the number of views acquired. Since only a fraction of the glandular tissue is irradiated, the mean glandular dose will be lower.

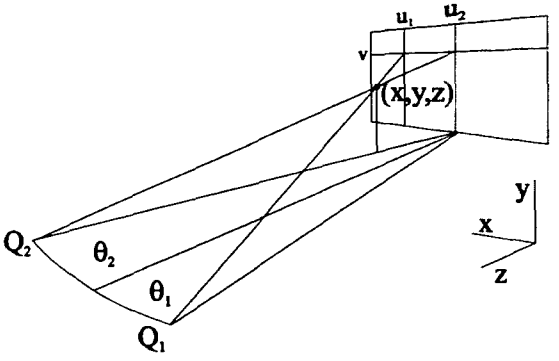

Figure 2: An illustration of the image acquisition geometry. When the x-ray tube is at position Q_1 the image of the calcification is projected onto the detector (dark gray) at a point (u_1,v), and at position Q_2 the image is projected to (u_2,v).

Currently, the calcifications in each image are identified manually. In this process, a human operator places a seed point near the center of a calcification. The calcification is then segmented semi-automatically using a recursive region-growing algorithm. Next, the corresponding projected image of the calcification is identified in the second view, and the calcification is segmented. These steps are repeated for every calcification for which correspondence between the views is found. This algorithm has been described in detail previously.[26,27]

It is possible to correlate the projected image of each calcification in the different views of the breast from the positions, shapes and sizes of the projected images. Note, for example, that the two projected positions $[(u_1, v)$ and $(u_2, v)]$ of a calcification at position (x,y,z) share a common coordinate, v, as shown in Figure 2. It is possible, therefore, to use the mass of the calcifications that span a similar range of v values to determine which projected shadow corresponds to which calcification in each view. By adding additional views, one can then verify the calculated 3-D position against the

segmented calcifications in those views, as well as identifying those calcifications, which are hidden or obscured in one or more of the other views. In this manner, it is possible to identify each calcification in each view.

We separately determine the *3-D location* and the *3-D shape* of each calcification. The 3-D location is determined geometrically. The 3-D shape of each calcification is determined using the segmented image data in conjunction with a simulated annealing reconstruction method. As illustrated in Figure 2, an object at point $C = (x,y,z)$ will produce a projection at $P_1 = (u_1,v)$ when viewed with the first x-ray source at point Q_1, and will produce a projection image at $P_2=(u_2,v)$ when viewed with the x-ray source at point Q_2. The line P_1Q_1 and P_2Q_2 lie in the plane Q_1Q_2C, and meet at the point C, which is the position of the calcification. These simple geometric considerations allow one to calculate the coordinates of C. A method for compensation of motion of the patient has also been developed.[29] When motion occurs, the lines P_1Q_1 and P_2Q_2 will not intersect. An affine transformation is determined by fitting the motion of obvious calcification pairs and then is applied to all calcifications being reconstructed.

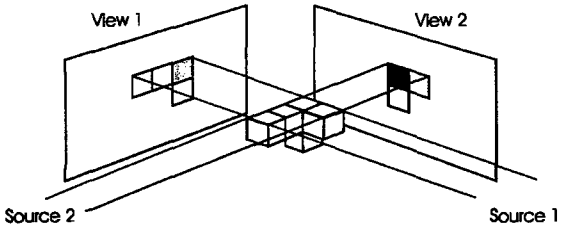

Figure 3: A simplified illustration of the reconstruction problem. An object (treated as a set of voxels containing calcium) is shown in two projections. Note that the intensity of the projection is related to the number of voxels traversed that contain calcium, and that the object is contained within the intersection of the back-projections (the image mask).

The intensity of the signal in each pixel of each view of the breast is dependent upon the amount of calcific material (and other breast tissues) in the path of the x-rays that contribute to signal at that pixel. This concept is illustrated in Figure 3, where a simulated object of equally attenuating cubes is held *in vacuo*, and imaged with an idealized imaging system in a non-divergent geometry. The intensity of the signal in the image depends upon the number of cubes traversed. To determine the 3-D shape of the object from the projection data requires an inverse transformation technique. We have chosen a simulated annealing method to which certain *a priori* constraints have been added. This method has also been described in detail previously.[26,27]

Once the list of voxels constituting the reconstruction of the calcification is obtained, the surface is approximated for the purpose of 3-D rendering using the marching cubes algorithm.[30] Rendering is performed using C and C++ with the OpenGL graphics library and X Windows. Objects are rendered in perspective with shading appropriate for both diffuse and specular reflection from both directional and diffuse light sources. The 3-D images may be viewed monoscopically or stereoscopically using CrystalEyes stereo eyewear.

2.3. Linear Tomosynthesis

In performing linear tomosynthesis, we again use our prone stereotactic biopsy system to acquire the projection image data set. For each tomosynthetic data set, fifteen images are acquired as the x-ray tube is moved through a 30 degrees arc; a clinically relevant geometry. As the x-ray focus is moved, the imaging plane **P** is held fixed. To perform a reconstruction, each x-ray image is viewed as a gray-scale function g_i defined on a region P_r of the imaging plane **P**, where i enumerates the x-ray exposure. For every plane **Q** parallel to **P** in which reconstruction will be performed, each projection position of the x-ray focus defines a one-to-one correspondence of points in the plane **Q** with the points in the plane **P**. Explicitly, for the i-th position of the x-ray tube, for each point q in **Q**, there is a line passing though the focus and q which meets **P** in a unique point p. Thus for every i there is a "projective" transformation between the points of **P** and **Q**. Further, the gray-scale function g_i on P_r can now be considered as a function g'_i defined in the region Q_i in the plane **Q**, and the value of the reconstructed gray scale image at a point q is the sum of all the g'_i which are defined at that point. As with conventional tomography, for objects lying within the plane **Q**, the functions g'_i add coherently to produce a well focused image, while for objects outside the plane are blurred. The advantage of synthetic tomography over conventional tomography is that the set of 15 or so images can be used to reconstruct multiple planes, while in conventional tomography each image would require an additional set of exposures.[31-33]

Typically we reconstruct the tomographic images in planar regions, Q_i, in 1 mm increments. These are rendered in X windows in a stack. One can use motion of the mouse to increment or decrement i thus allowing one to view the entire breast one slice at a time. It is also possible to window and level, and magnify the images.

3. RESULTS AND DISCUSSION

3.1. Stereoscopy

Stereoscopic images of the breast allow one to visualize the relative positions of objects in the breast. It is easier to appreciate this relationship in high contrast objects such as calcifications. In lower contrast objects, the relationship between the projections is less apparent. The method does allow one to understand how calcifications relate to the soft tissue stuctures of the breast.

We have found that it is more beneficial to render the constituent projection images of linear tomography data as stereoscopic pairs. In this way, you can view the breast at a variety of angles (typically covering 30° to 45° in 3° to 5° increments). Our viewing software allows us to double buffer stereoscopic images, and hence we can present smoothly rotating stereoscopic views of the breast. In this instance, the additional angular range of the image set allows one to determine with more confidence the relative relationship between different image features. Thus, an observer can build a better 3-D model of the breast in his or her mind. Unfortunately, there are dose considerations in using the linear tomographic projection data since these are typically acquired with a lower individual dose than true stereoscopic image pairs. The result is a lower SNR for any particular stereoscopic image pair, and hence the detection of certain objects such as very small calcifications will be adversely affected. We are currently evaluating this effect.

3.2. Limited View Reconstruction

3-D images of 44 cases of clustered calcification have been generated with the LVR method. Anecdotally, we have observed that in instances when the calcifications are associated with a mass, it has been possible to distinguish preferentially peripherally distributed calcifications from homogeneously distributed calcifications. This is possible in spite of the fact that in the 3-D renderings there is no frame of reference in which the reader can relate the calcifications to the mass. This observation is very important because preferentially peripherally distributed calcifications are predominately associated with benign diseases, while clustered malignant calcifications are more often homogeneously distributed. An example of a benign cluster of calcifications is shown in Figure 4. It has also been possible to elucidate the ductal distribution of some malignant calcifications using the 3-D reconstruction technique. An example of a malignant calcification cluster that demonstrates a ductal distribution is shown in Figure 5. In Figures 4 and 5, Figure a demonstrates a single digital mammographic views of the calcification cluster. The image depicts an area 2.5 cm x 2.5 cm. In Figures b and c, the calcifications that were segmented from each image are shown in two different views.

In our preliminary study of 44 cases, we compared the appearance of clustered calcifications in film-screen mammograms, digital 2-D mammograms and digital 3-D images. In the study, three radiologists separately reviewed each case. Fourteen of the cases were malignant, the remaining 30 cases were benign. In each case, the radiologist was asked to rate each case on a modified "degree of suspicion" scoring system; 5 = definitely malignant, 4 = probably malignant, 3 = suspicious for malignancy, 2 = probably benign, and 1 = definitely benign. A score of 3 or higher would indicate a biopsy procedure was necessary. With film images, the radiologist could use a magnifying glass or a hot-light if desired. In the case of the 2-D digital images, the readers were allowed to alter the display window and level and electronic magnification as desired. With the 3-D images, the radiologists could view the 3-D models from any angle.

The distribution of scores of the three radiologists is shown in Figure 6. As can be seen, the addition of the 2-D digital images and the 3-D images tended to shift the distribution of the benign scores lower, and the malignant scores higher. The accuracy of diagnosis rose from 36% for film to 63% adding 2-D digital images to 77% adding 3-D digital images; the latter representing a 210% improvement compared to film alone. The number of benign biopsies which would have been deemed necessary would have dropped from 28 for film alone to 16 using 2-D digital and 10 using 3-D data; a reduction of 66%.

3.3. Linear Tomosynthesis

We have not yet performed clinical linear tomosynthesis. Rather, the results of a preliminary phantom experiment are shown in Figure 7. The phantom consists of acrylic spheres contained in a water filled acrylic box. This box was superimposed upon a contrast-detail phantom. In Figure 7 (upper left), a projection image is shown. This image demonstrates the overlaying "clutter" of the spheres and cubes and effectively obscures most of the features of the contrast

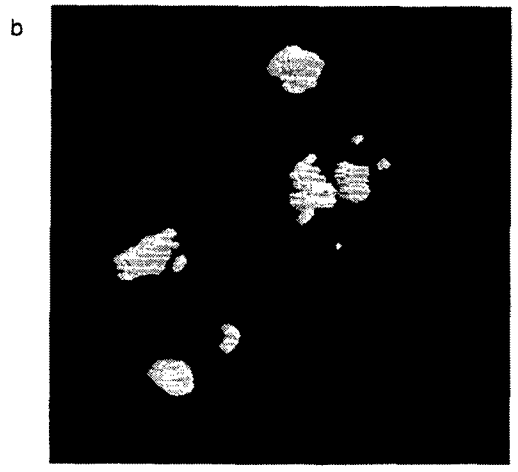

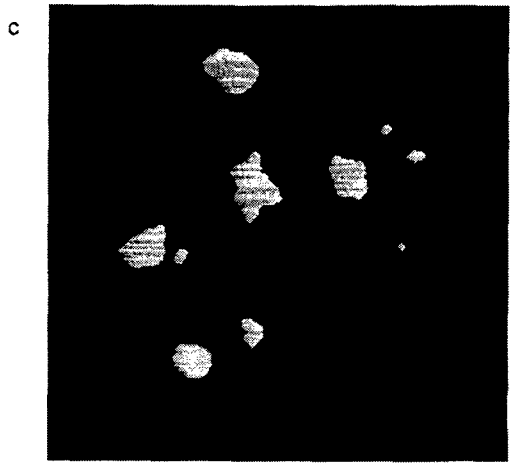

Figure 4: A radiograph of a benign cluster of calcifications (a). Also shown are 2 reconstructions of the cluster (b,c). The reconstructions show plate-like calcifications arranged in a spherical manner about a lucent center. This is typical of a fibroadenoma.

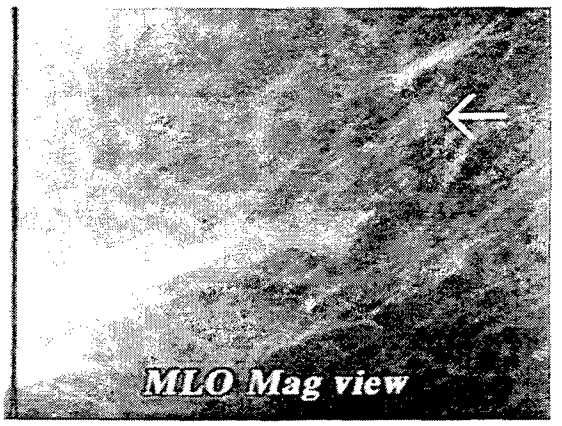

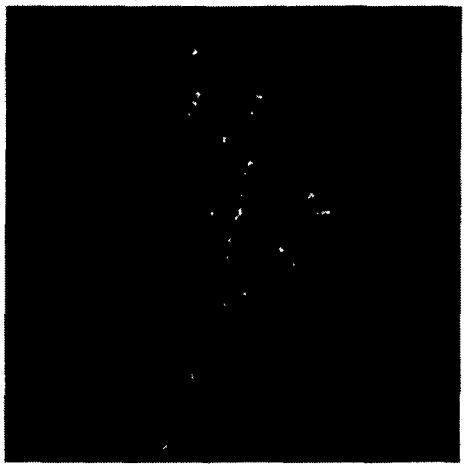

Figure 5: A radiograph of a malignant cluster of calcifications (a). Also shown are 2 reconstructions of the cluster (b,c). The reconstructions show a branching linear struction demonstrating ductal confinement of calcifications typical of a ductal carcinoma.

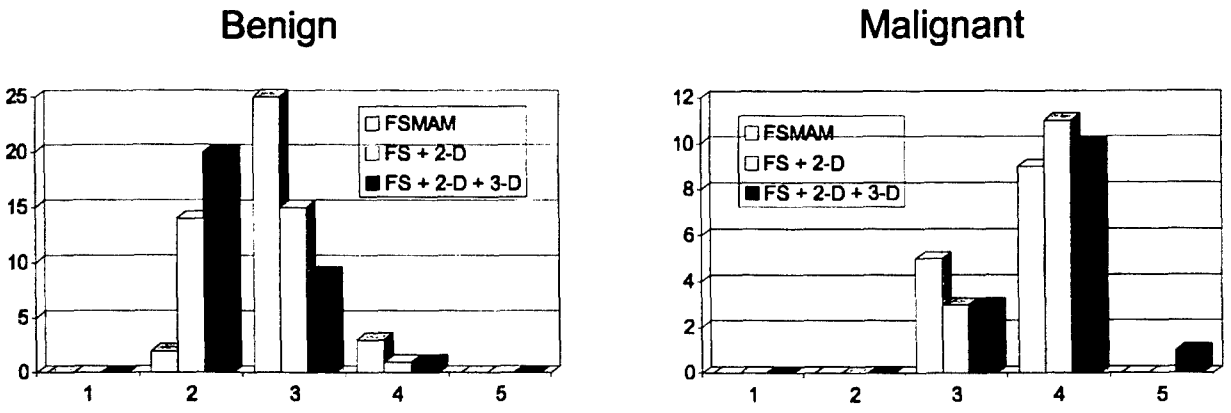

Figure 6: Histograms showing the number of benign and malignant cases rated with scores of 1 to 5. A score of 3 or greater would justify a biopsy.

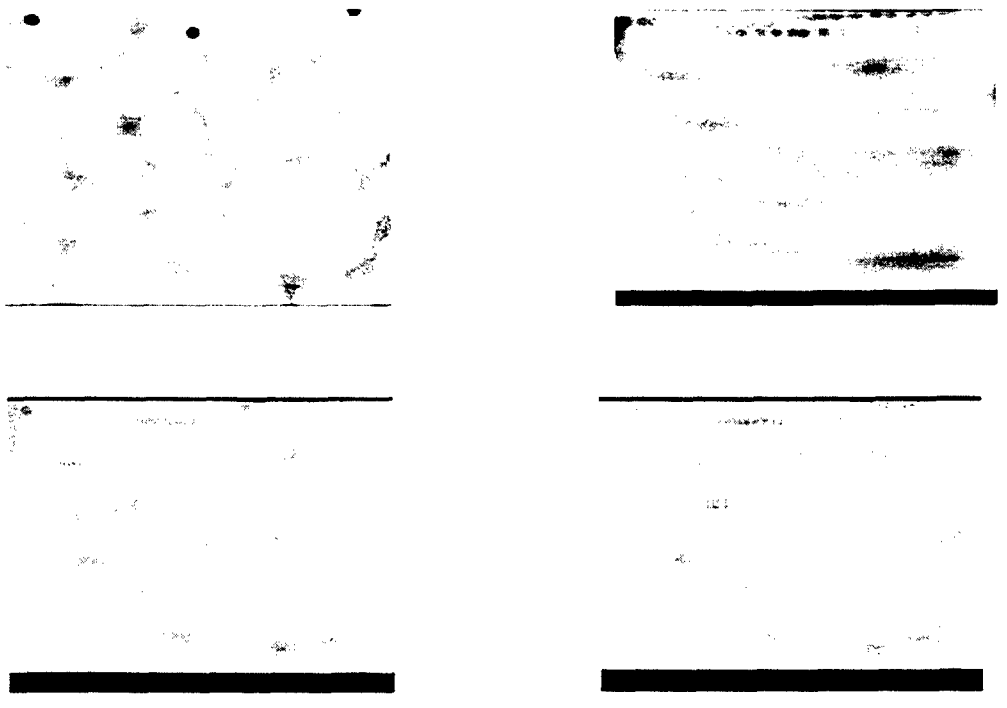

Figure 7: An tomosynthetic reconstruction of a phantom. The phantom consisted of a group of acrylic spheres and cubes immersed in water, and superimposed upon a contrast-detail phantom. A projection image is shown in the upper left. A slice through the contrast-detail phantom is shown in the upper right, clearly demonstrating more objects than are visible in the projection image. The lower images are reconstructed through slices which intersect the cubes and spheres.

detail phantom. Even at 10 times the dose this image was acquired at, we could not visualize more than 5 objects of the contrast-detail phantom. In Figure 7, we also show three reconstructions of the phantom. The lower images of Figure 7 are in the section containing the acrylic spheres. The upper right image of Figure 7, however, is in the plane containing the contrast-detail phantom. In this image, 24 contrast-detail elements are visible. The increase in detection of the objects is not related to the dose, but rather to the reduction in the overlaying clutter. Reduction of this structural noise results in an increase in the SNR of the contrast detail elements. It is hoped that similar improvements will be achieved by reducing the clutter of overlaying breast tissue and thus making subtle breast lesions more conspicuous.

4. CONCLUSIONS

In conclusion, we believe that existing digital mammography imaging systems should be used as an adjuvant tool to film-screen mammography. We have developed one such method that produces 3-D images of clustered mammary calcifications, and are investigating two more which place these calcifications in context with the surrounding tissues. These techniques use images that are acquired on a small field-of-view digital mammography prone stereotactic biopsy system. The LVR technique produces 3-D images using a method that includes identification, segmentation and correlation of each calcification in the breast in a limited number of projection images of the breast, and subsequent reconstruction of the calcifications from these views. Stereoscopic imaging of the breast requires fewer images but provides less depth perception. Linear tomosynthesis requires more images, but provides excellent depth perception, reducing overlaying clutter and making subtle lesions more conspicuous. The dose in each of these procedures is comparable to that used in magnification mammography. In a preliminary clinical evaluation, we have demonstrated that 3-D morphologic analysis of calcifications is possible and can significantly increase accuracy of diagnosis and decrease the number of benign biopsies required.

5. ACKNOWLEDGEMENTS

This research was supported by a grant from the RSNA Research and Education Fund, and is currently supported by the Department of Defense (DAMD17-96-1-6280 and DAMD17-97-1-7143). This work is conducted under the auspices of the International Digital Mammography Development Group. The authors wish to thank Dr. Stephen Feig, Dr. Catherine Piccoli, Dr. Steven Nussbaum, Dr. Elaine Wolk, and Ms. Lisa Fisher of Thomas Jefferson University for their assistance with this project.

6. REFERENCES

1. Seidman H *et al.* Survival experience in the Breast Cancer Detection Demonstration Project. *Ca.* **37**:258-290, 1987.
2. Feig SA. Decreased breast cancer mortality through mammographic screening: Results of clinical trials. *Radiology* **167**:659-665, 1988.
3. Shapiro *et al.* Current results of the breast cancer screening randomization trial: The Health Insurance Plan (HIP) of Greater New York, in NE Day and AB Miller (Eds) *Screening for Breast Cancer*, Toronto, Hogreofe, 1988.
4. Tabar L *et al.* Update of the Swedish two-county program for mammographic screening for breast cancer. *Radiol. Clin. N. Am.* **30**:187-210, 1992.
5. Kopans DB *et al.* Breast Imaging. *NEJM* **130**:960-967, 1984.
6. Sickles EA. Breast Imaging: A view from the present to the future. *Diagn. Imag. Clin. Med.* **54**:118-125, 1985.
7. Kopans DB. Non-mammographic breast imaging techniques. *Rad Clin N Am* **25**:961-971, 1987.
8. Kopans DB. Priorities for improved breast cancer imaging, in AG Haus and MJ Yaffe (eds) *Technical aspects of Breast Imaging*, RSNA, Oakbrook IL, 271-274, 1994.
9. Feig SA, Shaber GS, Patchefsky A, *et al.* Analysis of clinically occult and mammographically occult breast tumors. *AJR* 128:403-408, 1977.
10. Nishikawa RM *et al.* Scanned projection digital mammography. *Med Phys* **14**:717-727, 1987.
11. Maidment ADA. *Scanned-slot digital mammography*. PhD. Thesis, University of Toronto, Toronto, Canada, 1993.
12. Wolfe JN. Analysis of 462 breast carcinomas. *AJR* **121**: 846-853, 1974.
13. Frischbier H-J, Lohbeck HU. *Fruhdiagnostik des Mammakarzinoms*. Thieme, Stuttgart, 1977.

14. Bjurstam N. Radiology of the female breast and axilla. *Acta Radiol Suppl* **357, 1978**.
15. Menges V, Busing CM, Hirsch O. *RoFo* **135**:372-378, 1981.
16. Frankl G, Ackerman M. Xeromammography and 1200 breast cancers. *Radiol Clin North Am* **21**:81-91, 1983.
17. Moskowitz M. The predictive value of certain mammographic signs in screening for breast cancer. *Cancer* **51**:1007-1011, 1983.
18. Anderson I. Mammographic screening for breast carcinoma. Ph.D. Thesis , Malmo, 1980.
19. Murphy WA, DeSchryver-Kecskemeti K. Isolated clustered microcalcifications in the breast. *Radiology* **127**: 335-341, 1978.
20. Egan RL, McSweeney MB, Sewell CW. Intramammary calcifications without an associated mass in benign and malignant diseases. *Radiology* **137**:1-7, 1980.
21. Sickles EA. Further experience with microfocal spot magnification mammography in assessment of clustered breast microcalcifications. *Radiology* **137**:9-14, 1980.
22. Muir BB, Lamb J, Anderson TJ, *et al.* Microcalcification and its relationship to cancer of the breast. *Clin Radiol* **34**:193-200, 1983.
23. Sigfusson BF, Andersson I, Aspegren K, *et al.* Clustered breast calcifications. *Acta Radiologica* **24**: 273-281, 1983.
24. Lanyi M. *Diagnosis and Differential Diagnosis of Breast Calcifications.* Springer-Verlag, New York, 1988.
25. Robert N, Maidment ADA, and Yaffe MJ. Three-dimensional localization and display of breast microcalcifications. *Proceedings of the annual meeting division of medical and biological physics of the Canadian association of physics.* London Ontario, 1989.
26. Maidment ADA, Albert M, Conant EF and Feig SA. 3-D Mammary Calcification Reconstruction from a Limited Number of Views. *Proceedings of the SPIE*, **2708**, 378-389, 1996.
27. Maidment ADA, Conant EF, Feig SA, Piccoli CW and Albert M. Three-dimensional Analysis of Breast Calcifications in *Digital Mammography*, Excerpta Medica ICS-1119, Elsevier Sci., Holland, 245-250, 1996.
28. Limitation of Exposure to Ionizing Radiation. NCRP Report 116, Bethesda MD, 1993.
29. Albert M and Maidment ADA. Compensation for patient motion in stereotactic mammography. *Med. Phys.* **23** 1107, 1996.
30. Lorensen WE and Cline HE. Marching cubes: A high resolution 3D surface construction algorithm. *ACM Computer Graphics* **21**:163-169 1987.
42. Miller, E.R., McCurry, E.M., Hruka, B., An Infinite Number of Laminograms from a Finite Number of Radiographs, *Radiology*, 1971, 98 (249-255)
43. Grant, D.G. Tomosynthesis: a three dimensional radiographic imaging technique. *IEEE Trans. Biomed. Eng.*, 1972, 19 (20-28)
44. Ziedes des Plantes BG, Eine neue Methode zur Differenzierung in der Reontgenograpie (Panigraphie), *Acta. Radiol.* 1932, 13; 182-192 [Ger].

Digital Mammography

Nijmegen, 1998

Edited by

Nico Karssemeijer
Martin Thijssen
Jan Hendriks
and
Leon van Erning

Department of Radiology,
University Hospital Nijmegen,
Nijmegen, The Netherlands

KLUWER ACADEMIC PUBLISHERS
DORDRECHT / BOSTON / LONDON

THREE-DIMENSIONAL VISUALIZATION OF BREAST CANCER

ANDREW D.A. MAIDMENT, MICHAEL ALBERT,
EMILY F. CONANT AND STEPHEN A. FEIG.
Thomas Jefferson University, Department of Radiology,
Philadelphia, PA, USA

1. Introduction

Film-screen mammography is currently the most sensitive modality available for the early detection of breast cancer, yet it often fails to clearly indicate or contraindicate malignancy. As a result, many biopsies are performed, but only 1 in 4 biopsies result in the detection of cancer [1]. Biopsies represent a major expense and are a significant deterrent to women entering breast cancer screening programs. A definitive, non-invasive method of distinguishing benign and malignant breast lesions is essential.

We use small field-of-view digital mammography, with 3-D imaging methods to better distinguish malignant and benign lesions. The detection and differential diagnosis of subtle lesions using film-screen mammography is hindered by technical limitations, including insufficient film latitude, film granularity noise, and dose-inefficient scatter rejection [2]. Digital imaging can overcome these limitations. It has also been shown that differential diagnosis is limited by the processes of projection and superimposition that occur when any 2-D image is produced of a 3-D object [3]. The result is a loss of information regarding the structure and morphology of breast lesions. Lanyi has shown, using an invasive technique, that 3-D imaging of breast calcifications can overcome these limitations [3]. We have investigated three methods for 3-D imaging - stereoscopy, limited view reconstruction (LVR) and linear tomosynthesis.

2. Methodology for 3-D breast imaging

The greatest concern in acquiring 3-D images of the breast is the dose involved in acquiring images. The low energies used in mammography result in relatively high exposures (on the order of 1R entrance exposure per image for an average breast). To simply increase the number of views of the breast to acquire 3-D images is unacceptable. Care must be exercised to reduce the exposure for each view when acquiring 3-D images. For this reason computed tomography (CT) of the breast is not considered clinically viable. The three approaches discussed below demonstrate this tradeoff.

2.1. STEREOSCOPY

Most human observers perceive the world stereoscopically. The eyes of the observer are separated by approximately 10 cm causing binocular disparity, which incorporated with clues such as shading from different light sources allows the observer to determine the position of objects relative to one another in 3-D. Stereopsis can be simulated when radiographing the breast by acquiring images which are separated by 3° to 5° and are then displayed so that each eye views a different image. The images can each be acquired with a dose that is approximately 1/2 that used normally. We acquire images on a prone stereotactic breast biopsy system, fitted with a small field-of-view digital mammography detector that produces images which have a format of 1024 x 1024 pixels. The images are displayed stereoscopically by presenting the data alternately to the left and right eyes of observers wearing synchronized shuttered eyewear.

2.2. LIMITED VIEW RECONSTRUCTION

LVR was proposed by us to generate true 3-D images of breast calcifications, but without the high dose associated with conventional 3-D x-ray techniques such as CT. We still require relatively high dose projection images (comparable to non-grid film-screen mammography) to allow detection of the smallest possible calcifications within each projection image, but the technique requires few images (typically 3, maximum of 7). This technique is possible because the calcifications are reconstructed (from segmented image data), and a binary image reconstruction technique is employed.

The 3-D reconstruction of the calcification images is performed in a number of steps, beginning with acquisition of a limited number of projection images of the breast. Next, the calcifications are segmented from the background of breast parenchyma. The shape, size and position of each calcification in each view are used to determine the correspondence of the calcifications between the views. The 3-D location of each calcification is determined geometrically, and the 3-D shape of each calcification is derived using a simulated annealing approach. Finally, the images are rendered in 3-D. This method has been explained in detail previously [4-7].

2.3. LINEAR TOMOSYNTHESIS

In linear tomosynthesis, we use a prone stereotactic biopsy system to acquire 10-15 images in a 30 degrees arc. As the x-ray focus is moved, the imaging plane **P** is held fixed. To perform a reconstruction, each x-ray image is viewed as a gray-scale function g_i defined on a region P_r of the imaging plane **P**, where i enumerates the x-ray exposure. For every plane **Q** parallel to **P** in which reconstruction will be performed, each projection position of the x-ray focus defines a one-to-one correspondence of points in the plane **Q** with the points in the plane **P**. Explicitly, for the i-th position of the x-ray tube, for each point q in **Q**, there is a line passing though the focus and q which meets **P** in a unique point p. Thus for every i there is a "projective"

transformation between the points of **P** and **Q**. Further, the gray-scale function g_i on P_r can now be considered as a function g'_i defined in the region Q_i in the plane **Q**, and the value of the reconstructed gray scale image at a point q is the sum of all the g'_i which are defined at that point. As with conventional tomography, for objects lying within the plane **Q**, the functions g'_i add coherently to produce a well focused image, while for objects outside the plane are blurred. Synthetic tomography has the advantage that a single set of 10 to 15 images can be used to reconstruct an arbitrary number of planes, while in conventional tomography each plane would require an additional set of exposures. Typically we reconstruct the images in 1 mm increments.

3. Results and discussion

Stereoscopic images of the breast allow one to visualize the relative positions of objects in the breast. It is easier to appreciate this relationship in high contrast objects such as calcifications. We have found that it is beneficial to render the constituent projection images of linear tomography data as stereoscopic pairs. In this way, you can view the breast at a variety of angles (typically covering 30° to 45° in 3° to 5° increments). Our viewing software double buffers the stereoscopic images, hence we can present smoothly rotating stereoscopic views of the breast. In this instance, the additional angular range of the image set allows one to determine with more confidence the relationship between image features. Unfortunately, linear tomographic projection data are acquired with a lower individual dose than true stereoscopic image pairs. The result is a lower SNR for any particular stereoscopic image pair, and hence the detection of certain objects such as very small calcifications will be adversely affected

3-D images of 44 cases of clustered calcification have been generated with the LVR method. Anecdotally, we have observed that when the calcifications are associated with a mass, it has been possible to distinguish preferentially peripherally distributed calcifications from homogeneously distributed calcifications. Preferentially peripherally distributed calcifications are predominately associated with benign diseases, while clustered malignant calcifications are more often homogeneously distributed.

We compared the appearance of clustered calcifications in film-screen mammograms, digital 2-D mammograms and digital 3-D images. Three radiologists separately reviewed each case. Fourteen of the cases were malignant; the remainding 30 cases were benign. The radiologist rated each case on a "degree of suspicion" scoring system; 5 = definitely malignant, 4 = probably malignant, 3 = suspicious for malignancy, 2 = probably benign, and 1 = definitely benign. A score of 3 or higher would indicate a biopsy was necessary. We observed that the addition of 2-D digital images and the 3-D images tended to shift the distribution of the benign scores lower, and the malignant scores higher. The accuracy of diagnosis (diagnosis from image equals biopsy results/total number of cases) rose from 36% to 63% to 77%. The number of benign biopsies which would have been deemed necessary would have dropped from 28 for film to 16 using 2-D digital and 10 using 3-D data, a reduction of 66%.

We have not yet performed tomosynthesis clinically. Rather, we have performed phantom studies. The phantoms consist of acrylic spheres contained in a water filled acrylic box. This box was superimposed upon a contrast detail phantom. Images of this phantom demonstrate an overlaying "clutter" of spheres and cubes which effectively obscures the features of the contrast detail phantom. In projection images, we could not visualize more than 5 objects of the contrast detail phantom. In tomographic reconstructions of the phantom, all 24 contrast detail elements are visible. The increase in detection of the objects is not related to the dose, but rather to the reduction in the overlaying clutter. Reduction of this structural noise results in an increase in the SNR of the contrast detail elements. It is hoped that similar improvements will be achieved by reducing the clutter of overlaying breast tissue and thus making subtle breast lesions more conspicuous.

4. Conclusions

In conclusion, we believe that existing digital mammography imaging systems should be used as an adjuvant tool to film-screen mammography. We have developed three methods which based upon a small field-of-view digital biopsy system. The LVR technique produces 3-D images using a method that includes identification, segmentation and correlation of each calcification in the breast in a limited number of projection images of the breast, and subsequent reconstruction of the calcifications from these views. Stereoscopic imaging of the breast requires fewer images but provides less depth perception. Linear tomosynthesis requires more images, but provides excellent depth perception, reducing overlaying clutter and making subtle lesions more conspicuous. The dose in each of these procedures is comparable to that used in magnification mammography. In preliminary clinical evaluation we have demonstrated that 3-D morphologic analysis of calcifications is possible and can significantly increase accuracy of diagnosis and decrease the number of benign biopsies required.

References

[1] Feig SA, Shaber GS, Patchefsky A, *et al.* Analysis of clinically occult and mammographically occult breast tumors. *AJR* 128:403-408, 1977.

[2] Nishikawa RM *et al.* Scanned projection digital mammography. *Med Phys* **14**:717-727, 1987.

[3] Lanyi M. *Diagnosis and Differential Diagnosis of Breast Calcifications.* Springer-Verlag, New York, 1988.

[4] Robert N, Maidment ADA, and Yaffe MJ. Three-dimensional localization and display of breast microcalcifications. *Proceedings of the annual meeting division of medical and biological physics of the Canadian association of physics.* London Ontario, 1989.

[5] Maidment ADA, Albert M, Conant EF and Feig SA. 3-D Mammary Calcification Reconstruction from a Limited Number of Views. *Proceedings of the SPIE*, **2708**, 378-389, 1996.

[6] Maidment ADA, Conant EF, Feig SA, Piccoli CW and Albert M. Three-dimensional Analysis of Breast Calcifications in *Digital Mammography*, Excerpta Medica ICS-1119, Elsevier Sci., Holland, 245-250, 1996.

[7] Maidment ADA, Albert M, Conant EF. Three-dimensional imaging of breast calcifications. *Proceedings of the SPIE*, **3240**, 200-208,1997.